of canine distemper virus in Vero cells expressing canine SLAM (CD150) and their adaptability to marmoset B95a cells. J. Virol. 77:9943–9950.
17. **Singethan K, et al.** 2006. CD9-dependent regulation of canine distemper virus-induced cell-cell fusion segregates with the extracellular domain of the haemagglutinin. J. Gen. Virol. **87**:1635–1642.
18. **Tahara M, et al.** 2008. Measles virus infects both polarized epithelial and immune cells by using distinctive receptor-binding sites on its hemagglutinin. J. Virol. **82**:4630–4637.
19. **Takasu T, et al.** 2003. A continuing high incidence of subacute sclerosing panencephalitis (SSPE) in the Eastern Highlands of Papua New Guinea. Epidemiol. Infect. **131**:887–898.
20. **Takeda M, Tahara M, Nagata N, Seki F.** 2011. Wild-type measles virus is intrinsically dual-tropic. Front. Microbiol. **2**:279.
21. **van Moll P, Alldinger S, Baumgartner W, Adami M.** 1995. Distemper in wild carnivores: an epidemiological, histological and immunocytochemical study. Vet. Microbiol. **44**:193–199.
22. **von Messling V, Milosevic D, Cattaneo R.** 2004. Tropism illuminated: lymphocyte-based pathways blazed by lethal morbillivirus through the host immune system. Proc. Natl. Acad. Sci. U. S. A. **101**:14216–14221.
23. **Wang L-F, et al.** 2012. Family *Paramyxoviridae*, p 672–685. *In* King AMQ, Adams MJ, Carstens EB, Lefkowitz EJ (ed), Virus taxonomy, 9th ed. Elsevier Academic Press, London, United Kingdom.

Journal of Virology

Functional and Structural Characterization of Neutralizing Epitopes of Measles Virus Hemagglutinin Protein

Maino Tahara, Yuri Ito, Melinda A. Brindley, Xuemin Ma, Jilan He, Songtao Xu, Hideo Fukuhara, Kouji Sakai, Katsuhiro Komase, Paul A. Rota, Richard K. Plemper, Katsumi Maenaka and Makoto Takeda

J. Virol. **2013, 87(1):666. DOI: 10.1128/JVI.02033-12.**
Published Ahead of Print 31 October 2012.

JVI
Journals.ASM.org

Functional and Structural Characterization of Neutralizing Epitopes of Measles Virus Hemagglutinin Protein

Maino Tahara,[a] Yuri Ito,[b] Melinda A. Brindley,[c] Xuemin Ma,[a] Jilan He,[a] Songtao Xu,[a] Hideo Fukuhara,[b] Kouji Sakai,[a] Katsuhiro Komase,[a] Paul A. Rota,[d] Richard K. Plemper,[c] Katsumi Maenaka,[b] Makoto Takeda[a]

Department of Virology 3, National Institute of Infectious Diseases, Tokyo, Japan[a]; Laboratory of Biomolecular Science, Faculty of Pharmaceutical Sciences, Hokkaido University, Hokkaido, Japan[b]; Department of Pediatrics, Emory University School of Medicine, Atlanta, Georgia, USA[c]; Measles, Mumps, Rubella and Herpesviruses Laboratory Branch, Division of Viral Diseases, Centers for Disease Control and Prevention, Atlanta, Georgia, USA[d]

Effective vaccination programs have dramatically reduced the number of measles-related deaths globally. Although all the available data suggest that measles eradication is biologically feasible, a structural and biochemical basis for the single serotype nature of measles virus (MV) remains to be provided. The hemagglutinin (H) protein, which binds to two discrete proteinaceous receptors, is the major neutralizing target. Monoclonal antibodies (MAbs) recognizing distinct epitopes on the H protein were characterized using recombinant MVs encoding the H gene from different MV genotypes. The effects of various mutations on neutralization by MAbs and virus fitness were also analyzed, identifying the location of five epitopes on the H protein structure. Our data in the present study demonstrated that the H protein of MV possesses at least two conserved effective neutralizing epitopes. One, which is a previously recognized epitope, is located near the receptor-binding site (RBS), and thus MAbs that recognize this epitope blocked the receptor binding of the H protein, whereas the other epitope is located at the position distant from the RBS. Thus, a MAb that recognizes this epitope did not inhibit the receptor binding of the H protein, rather interfered with the hemagglutinin-fusion (H-F) interaction. This epitope was suggested to play a key role for formation of a higher order of an H-F protein oligomeric structure. Our data also identified one nonconserved effective neutralizing epitope. The epitope has been masked by an *N*-linked sugar modification in some genotype MV strains. These data would contribute to our understanding of the antigenicity of MV and support the global elimination program of measles.

Measles virus (MV) used to be a major cause of death in children. The WHO estimated that ~4% of deaths in children under 5 years of age were caused by measles during the period from 2000 to 2003 (1). However, effective vaccination programs have eliminated measles in the Western Hemisphere, and several other countries are approaching measles elimination (2). In the last decade, the number of measles-related deaths was reduced by more than 90% in all WHO regions, except for Southeast Asia (2). This year, the Measles and Rubella Initiative (http://www.measlesinitiative.org/) developed the Global Measles and Rubella Strategic Plan 2012–2020, which aims to reduce global measles mortality by at least 95% compared with 2000 by the end of 2015 and to achieve measles elimination in at least five WHO regions by the end of 2020. One of the factors favoring measles eradication is the monotypic nature of MV. All the available data suggest that measles eradication is biologically feasible (3, 4). However, a biochemical, molecular, and virological basis for the monotypic nature of MV remains to be provided.

MV is an enveloped virus in the genus *Morbillivirus* of the family *Paramyxoviridae* and possesses two types of glycoprotein spikes, the hemagglutinin (H) and fusion (F) proteins, on the viral envelope. The H protein is responsible for binding to cellular receptors on the target host cells. The signaling lymphocyte activation molecule (SLAM) expressed on immune system cells and nectin4 expressed at adherens junctions in epithelia function as the principal receptors for MV (5–8). Binding of the H protein to a receptor triggers F protein-mediated membrane fusion between the virus envelope and the host cell plasma membrane. Although neutralizing Abs directed against each of the viral envelope glycoproteins are elicited, H protein-specific Abs mainly account for the protection against MV infection (9–11). All measles vaccines consist of live attenuated MV strains isolated about a half a century ago. Currently, 24 genotypes are recognized for MV, and all vaccine strains belong to the same single genotype (genotype A) (12). To date, measles vaccines have been effective, despite differences in the endemic genotypes present in different countries or regions. Consequently, based on these observations, there is no evidence to suggest that MV undergoes a major antigenic drift. Nevertheless, several studies have suggested that currently circulating MV strains show antigenic variations, which could potentially affect the efficacy of vaccination (4, 13–17). Many amino acid residues have been documented to constitute a portion of an epitope. The data show that the H protein has several neutralizing epitopes (NEs), which may locate at the receptor-binding site (RBS) or a region interacting with the F protein. A list of amino acids or regions, which may constitute an epitope, and Abs, which recognize these epitopes, has been provided by Bouche et al. (10). Recently, Hashiguchi et al. determined a crystal structure of the head domain of the H protein in complexes with the V domain of SLAM (18). The head domain of the H protein is formed with six β-sheets arranged in a six-bladed propeller fold (19). SLAM binds to a β-sheet using the side of the propeller fold structure (18). The

Received 4 August 2012 Accepted 22 October 2012
Published ahead of print 31 October 2012
Address correspondence to Maino Tahara, maino@nih.go.jp.
Supplemental material for this article may be found at http://dx.doi.org/10.1128/JVI.02033-12.

doi:10.1128/JVI.02033-12

H protein head forms a homodimer, which is further assembled into a tetrameric structure by forming a dimer of dimers (18). These data allowed us to conduct a fine characterization of epitopes on the H protein. In the present study, we identified the location of several neutralizing epitopes on the MV H protein structure, and characterized these epitopes, providing a molecular basis for the sustainability of the monotypic nature of MV.

MATERIALS AND METHODS

Cells. II-18 (20) and B95a (21) cells were maintained in RPMI medium (Invitrogen) supplemented with 7.5% fetal calf serum (FCS). BHK/T7-9 cells constitutively expressing T7 RNA polymerase (22) were maintained in E-MEM (Invitrogen) supplemented with 10% tryptose phosphate broth and 5% FCS. Vero and Vero/hSLAM cells (Vero cells constitutively expressing human SLAM) (23) were maintained in DMEM (GIBCO) supplemented with 7.5% FCS.

MAbs. Mouse monoclonal antibodies (MAbs) (A2, A26, B5, B12, E39, E81, E103, E128, and E185) were raised against the H protein of the Toyoshima MV strain (genotype A), and some of them were reported previously (24–26). Competitive binding enzyme-linked immunosorbent assays (ELISAs) were performed as reported previously (25). Briefly, peroxidase-conjugated B5, B69, B12, A2, A26, or C149 MAb was mixed with various dilutions of an unlabeled MAb (B5, E81, E128, E185, E39, or E103) and then allowed to react with the MV antigen-coated wells for 2 h. The binding of the peroxidase-conjugated MAb to the MV antigens was detected as described previously (27).

Plasmid construction. All full-length genome plasmids were derived from the p(+)MV323 plasmid encoding the antigenic full-length cDNA of the IC-B strain (genotype D3) (28). The p(+)MV323-Luci plasmid, which has an additional transcriptional unit for the *Renilla* luciferase gene, was reported previously (24). The full-length genome plasmids encoding the H gene of different genotype strains were generated by replacing the H gene region of p(+)MV323-Luci with the corresponding cDNA for the Edmonston-tag [A] (29), MVi/Massachusetts.USA/26.09[B3], MVi/New York.USA/22.09[D4], MVi/Vietnam/29.01[D5], MVi/Okinawa.JPN/37.09[D8], MVi/California.USA/5.9[D9], and MVi/Pennsylvania.USA/20.09[H1] strains. Point mutations, Q391R and Q311R, were introduced into the H gene region of p(+)MV323-Luci by site-directed mutagenesis. Similarly, G211S, E235G, Y252H, L284F, L296F, and G302R mutations were independently introduced into the H gene region of p(+)MV323-Ed/H-Luci (plasmid for the IC/Ed-H-Luci virus) (24).

Viruses. IC323-EGFP, IC323-Luci, IC/EdH-EGFP, IC/EdH-Luci, MV323-EGFP-H-β12(N481Y), MV323-EGFP-H8, -H9, -H10, and -H11 were reported previously (24, 30–32). Other recombinant MVs were generated from the respective full-length genome plasmid as reported previously (33).

Neutralizing assay. A suspension of recombinant MV (2,000 PFU per 75 μl) was incubated with serially diluted MAbs for 30 min at 37°C (the first dilution of each MAb was 1:10, followed by 2-fold dilutions). After incubation with the MAb, the virus solution was inoculated into culture media of confluent monolayers of II-18 (nectin4$^+$) and B95a (SLAM$^+$) cells. For recombinant viruses possessing the genotype A H gene (genotype A viruses; IC/EdH-Luci and IC/EdH-EGFP) and their mutants, CD46-dependent infection was blocked by a MAb against CD46 (clone M75) when the assay was performed with II-18 cells. At 2 days postinfection, the luciferase activity in the cells was measured using a Dual-Glo luciferase assay system (Promega). The neutralizing titer was indicated by the maximum dilution point, exhibiting >50% reduction of luciferase activity. The amount of Ig in each MAb solution (mouse ascites) was analyzed by an ELISA that detects the Fc region of Ig (TaKaRa). The neutralizing titers were normalized by the amount of Ig and are shown in the tables. When enhanced green fluorescent protein (EGFP)-expressing recombinant MVs were used for neutralizing assays, monolayers of II-18 and B95a cells in 24-well cluster plates were incubated with neutralized virus samples for 1 h at 37°C. After a 1-h incubation, 200 μl of RPMI medium supplemented with 7.5% fetal bovine serum (FBS) and 100 μg/ml fusion-blocking peptide (Z-D-Phe-Phe-Gly) (Peptide Institute Inc., Osaka, Japan) was added to each well to block a second round of infection by progeny viruses. At 48 h postinfection, the number of EGFP-expressing cells was counted under a fluorescence microscope. The cell number was expressed in cell infectious units (CIU). The number of CIU for each recombinant MV was also determined in the absence of the Ab and compared with that in the presence of the Ab. The number of CIU for each virus without the Ab was set to 100%.

Ab-selected escape mutants. Recombinant MVs (IC323-EGFP and IC/EdH-EGFP) were incubated with a MAb (B5, E81, or E103) (the Ig concentrations were 0.5 to 1.4 mg/ml) for 30 min at 37°C and then propagated in B95a or II-18 cells in the presence of the MAb. At 2 days postinfection, several syncytia expressing EGFP were independently picked up, suspended in a small volume (100 μl) of culture medium, incubated with the respective MAb for 30 min at 37°C, and then cultured with fresh cells. This cycle was repeated twice, and the H gene nucleotide sequences of the selected mutants were determined as reported previously (33).

Replication kinetics. II-18 cells on 6-well plates were infected with recombinant MVs at a multiplicity of infection (MOI) of 0.01 per cell. After various time intervals, cells were harvested with culture medium and determined for their CIU on Vero/SLAM cells (23).

H and F protein coimmunoprecipitation. Monolayers of Vero cells on 6-well plates were transfected with 3 μg of pCG-EdmHn3xFLAG (Edmonston H protein containing an N-terminal triple Flag tag) (34) and 3 μg of pCG-EdmFc2xHA (Edmonston F protein containing a C-terminal double hemagglutinin [HA] tag) (35) in the presence of 100 μM fusion inhibitory peptide. MV H and F protein coimmunoprecipitation was performed as described previously (36). A mixture of CV1/CV4 MAbs (Millipore) served as a reference (1:1,000). MAbs B5, E81, E103, and E128 were used at a dilution of 1:2,000.

H and H-(473-477A) protein immunoprecipitation. Vero cells on 6-well plates were transfected with 6 μg of pCG-EdmHn3xFLAG or pCG-EdmH473-477An3xFLAG (37). At 36 h posttransfection, the cells were lysed in M2 lysis buffer (50 mM Tris-HCl [pH 7.4], 150 mM NaCl, 1 mM EDTA, 1% Triton X-100, protease inhibitors [Roche], 1 mM phenylmethylsulfonyl fluoride [PMSF]), cleared by centrifugation for 30 min at 20,000 × *g* and 4°C, and incubated with MV H protein ectodomain Abs (CV1/CV4 at 1:1,000 or E128 at 1:2,000). Immunoprecipitation, gel fractionation, and detection of Flag-tagged H protein antigenic material was performed as described previously (34).

Pulse-labeling and immunoprecipitation of MV proteins. At 36 h postinfection, Vero/hSLAM cells infected with recombinant MVs were cultured in methionine-cysteine-deficient medium for 1 h, pulse-labeled with [^{35}S]methionine-cysteine using EasyTag EXPRE35S35S protein labeling mix (PerkinElmer), and then lysed in radioimmunoprecipitation assay (RIPA) buffer. Polypeptides in the cell lysate were immunoprecipitated with a rabbit polyclonal Ab raised against the Toyoshima MV strain and analyzed by SDS-PAGE as reported previously (38). For endoglycosidase H (Endo-H) digestion, immunoprecipitated samples were eluted in 50 mM Tris-HCl (pH 7.4) containing 0.5% SDS by boiling for 4 min. The supernatants were then mixed with 0.1 M sodium citrate buffer (pH 5.3) containing Endo-H and incubated overnight at 37°C.

Surface plasmon resonance assay. Surface plasmon resonance assays were performed using a Biacore 3000 (GE Healthcare) as reported previously (19). Briefly, the biotinylated H protein head domain was immobilized using a biotin capture kit (GE Healthcare) at 400 response units for binding experiments. A solution including each MAb was applied to the chip at a saturated state. Next, soluble human SLAM ectodomain comprising the N-terminal Ig V set domain tandemly connected to the corresponding Ig C2 set domain of mouse SLAM, which largely improves the protein stability, was placed on the chip at a flow rate of 10 ml/min at 25°C. Biotinylated bovine serum albumin (BSA) was used as a negative control. It was difficult to determine the proper regeneration conditions, because the immobilized MV H protein head domain was not as stable under

TABLE 1 Summary of competitive binding ELISAs of anti-H protein MAbs

Unlabeled Ab[a]	Antigenic site	Antigenic site, peroxidase-labeled Ab[b]					
		I, B5[a]	*I*, B69	*I*, B12	*II*, A2	*II*, A26	*III*, C146
B5	*I*	++	++	++	−	+	−
E81	*I*	++	++	++	−	−	−
E128	*II*	−	−	−	++	−	−
E185	*iv*	−	−	−	−	−	+
E39	*v*	−	−	+	−	−	−
E103	*vi*	−	−	−	−	−	−

[a] MAbs used for neutralizing assays in the present study.
[b] ++, complete inhibition; +, partial inhibition; −, no inhibition.

typical regeneration conditions, such as acidic pH, basic pH, or other organic solutions. Therefore, we immobilized the same level of the H protein head domain for each binding experiment.

RESULTS

Antigenic sites *I*, *II*, and *vi* are effective neutralizing epitopes, and all except antigenic site *II* are conserved among different genotypes. In 1985, Sato et al. (25) reported various sets of MAbs against MV structural proteins. In the study, 11 MAbs recognizing the H protein were characterized in detail. Based on competitive ELISA data, three nonoverlapping or partially overlapping antigenic sites (*I*, *II*, and *III*) in the H protein were predicted (25). In addition to these 11 MAbs, we analyzed a further five MAbs (E81, E128, E185, E39, and E103) directed against the H protein by competitive binding ELISAs (Table 1). E81 and E128 completely inhibited the binding of MAbs recognizing antigenic sites *I* and *II*, respectively (Table 1). On the other hand, neither E185, E39, nor E103 showed complete inhibition against the binding of MAbs recognizing antigenic sites *I*, *II*, and *III*. E39 and E185 only partially inhibited the binding of MAbs recognizing antigenic sites *I* and *III*, respectively (Table 1). E103 showed no competitive inhibition against the binding of MAbs recognizing antigenic sites *I*, *II*, and *III*. Based on these data, we tentatively predicted antigenic sites *iv*, *v*, and *vi*, which were recognized by E185, E39, and E103, respectively (Table 1). The newly tested MAbs (E81, E128, E185, E39, and E103) and B5 reported by Sato et al. (25) were then used for MV neutralizing assays. The antigenic site recognized by each MAb is shown in parentheses: B5(*I*), E81(*I*), E128(*II*), E185(*iv*), E39(*v*), and E103(*vi*). Eight distinct recombinant MVs were used as neutralization targets (Table 2; see also Table S1 in the supplemental material). These recombinant MVs were based on the IC323 genomic background and encoded a *Renilla* luciferase reporter gene and an H gene derived from different MV genotypes (A, B3, D3, D4, D5, D8, D9, and H1) (see Table S1) (28, 39). They were named on the basis of the genotype of the H gene: genotype A, B3, D3, D4, D5, D8, D9, and H1 viruses. MAbs B5(*I*), E81(*I*), E128(*II*), and E103(*vi*) showed high neutralizing titers in SLAM$^+$ B95a and/or nectin4$^+$ II-18 cells (20, 21). While B5(*I*), E81(*I*), and E103(*vi*) neutralized all of the MV genotypes tested, E128(*II*) was only effective against genotype A, B3, D8, and H1 viruses (Table 2). The neutralizing titers of E185(*iv*) and E39(*v*) were significantly lower than those of B5(*I*), E81(*I*), E128(*II*), and E103(*vi*) (Table 2). These data suggest that antigenic sites *I*, *II*, and *vi* are effective neutralizing epitopes and that, with the exception of antigenic site *II*, all epitopes are conserved among the different MV genotypes.

Antigenic site *I* is located near the RBS, while antigenic site *vi* is located at a position distant from the RBS. To identify the locations of antigenic sites on the H protein, EGFP-expressing

TABLE 2 Neutralizing titers against MV strains possessing H genes from different genotypes

Cell line	Genotype, year isolated	Neutralizing titer against recombinant MV strain[a]:					
		B5(*I*)	E81(*I*)	E128(*II*)	E185(*iv*)	E39(*v*)	E103(*vi*)
B95a	A, 1954	30,144	863	1,968	494	<27	2,558
	B3, 2009	60,288	1,727	1,968	987	<27	10,231
	D3, 1984	7,536	1,727	15	31	<27	10,231
	D4, 2009	30,144	1,727	31	62	<27	20,462
	D5, 2001	30,144	863	15	494	<27	10,231
	D8, 2009	60,288	1,727	1,968	987	<27	20,462
	D9, 2010	60,288	1,727	15	987	<27	20,462
	H1, 2009	30,144	1,727	1,968	494	<27	20,462
II-18	A, 1954	30,144	27,631	62,977	124	1,750	10,231
	B3, 2009	30,144	27,631	62,977	1,974	1,750	10,231
	D3, 1984	3,768	27,631	123	62	<27	20,462
	D4, 2009	30,144	27,631	31	<8	<27	10,231
	D5, 2001	30,144	27,631	<4	1,974	<27	20,462
	D8, 2009	60,288	27,631	62,977	987	<27	10,231
	D9, 2010	60,288	27,631	123	1,974	<27	10,231
	H1, 2009	15,072	13,815	62,977	494	1,750	10,231

[a] Neutralizing titers for 1 mg/ml of Ig.

TABLE 3 Neutralizing titers against recombinant MVs possessing the H protein of genotye D3 virus with amino acid substitutions

Cell line	Mutation	Neutralizing titer against recombinant MV[a]: B5(*I*)	E81(*I*)	E103(*vi*)
B95a	wt: (−)	7,536	1,727	10,231
	Q391R	<471	<14	20,462
	Q311R	1,884	1,727	80
II-18	wt: (−)	3,764	27,631	20,462
	Q391R	<4	<3	20,462
	Q311R	1,884	27,631	20

[a] Neutralizing titers for 1 mg/ml of Ig.

MVs (IC323-EGFP) (30) that escaped from neutralization were isolated, and the amino acid changes in the H protein were identified by sequence analysis. Of the two escape mutants obtained, one escaped from neutralization by E81(*I*) through a Q391R mutation, and the other escaped E103(*vi*) through a Q311R mutation. These mutations were rebuilt in the luciferase gene-encoding recombinant IC323-Luci genome (24) by site-directed mutagenesis and reverse genetics (see Table S1 in the supplemental material). The resulting IC323-Luci-H(Q391R) was largely resistant to B5(*I*) but neutralized by E103(*vi*) with similar efficiency to that found for the parental virus (Table 3). The IC323-Luci-H(Q311R) recombinant was neutralized efficiently by B5(*I*) and E81(*I*) but escaped from neutralization by E103(*vi*) (Table 3). The amino acid residues at positions 391 and 311 are located within previously recognized epitopes on the H protein (10, 18, 19), which apparently correspond to antigenic sites *I* and *vi* (Fig. 1B and Table 4). The amino acid changes observed in the escape mutants indicate that antigenic site *I* is located near the SLAM-binding site, while antigenic site *vi* is located at a more distal position, although both act as effective neutralizing epitopes (Fig. 1B and Table 2). Mutagenesis of the H protein confirmed that the nectin4-binding site is distinct from the SLAM-binding site but probably shows a partial overlap (32, 40). This is consistent with the neutralization of MV by B5(*I*) and E81(*I*) on II-18 cells (Table 2). Epitope *vi* recognized by E103 corresponds to the previously predicted epitope recognized by BH38 and I-29 (Table 4) (10, 41, 42). Importantly, H mutants with Q391R or Q311R replicated somewhat less efficiently than the parental virus in cultured cells (Fig. 2), suggesting conformational effects of these changes on the H protein structure.

Antigenic site *II* is located near the bottom surface of the H protein head domain and is shielded by *N*-glycans attached to residue 416 in recent outbreak strains of MV. As described above, E128(*II*) neutralized several MV genotypes but failed to neutralize genotype D3, D4, D5, and D9 viruses (Table 2). Comparison of the H protein sequences of various MV genotypes indicated that the H proteins of MV genotypes D3, D4, D5, and D9, but not of genotypes A, B2, D8, and H1, harbor an additional potential site for *N*-linked glycosylation at residue 416 (see Fig. S1 in the supplemental material) (17, 43, 44). The electrophoretic mobility of the H proteins of genotype D3, D4, D5, and D9 was markedly reduced compared with that of the H proteins of genotypes A, B3, D8, and H1 (Fig. 3A), suggesting that an additional *N*-glycan moiety may be present on the H proteins of the former genotypes. Follow-up analyses with recombinant MV variants featuring a chimeric H gene combining fragments of the IC323 (genotype D3) and Edmonston (genotype A) strains (see Table S1) (31) showed that the amino acid difference at position 416 served as a determinant for the differential response to neutralization by E128(*II*) (Fig. 2B and C and Table 5). The addition of an *N*-glycan was confirmed by endoglycosidase H (Endo-H) treatment (Fig. 3D) as reported previously (17). In addition, the H protein of the Edmonston strain entirely lost its reactivity with E128(*II*) when carrying amino acid substitutions at positions 473 to 477 (Fig. 3E) (34). The epitope *II* likely constitutes a portion of RBS, since the amino acid region at positions 473 to 477 is involved in interaction with CD46, a receptor for MV vaccine strains (10, 45). Taken together, these data underscore that the *N*-glycan at position 416 masked epitope *II*, one of the major antigenic sites, which is located in the vicinity of a CD46-binding site (Fig. 1C). However, it was previously reported that serum samples derived

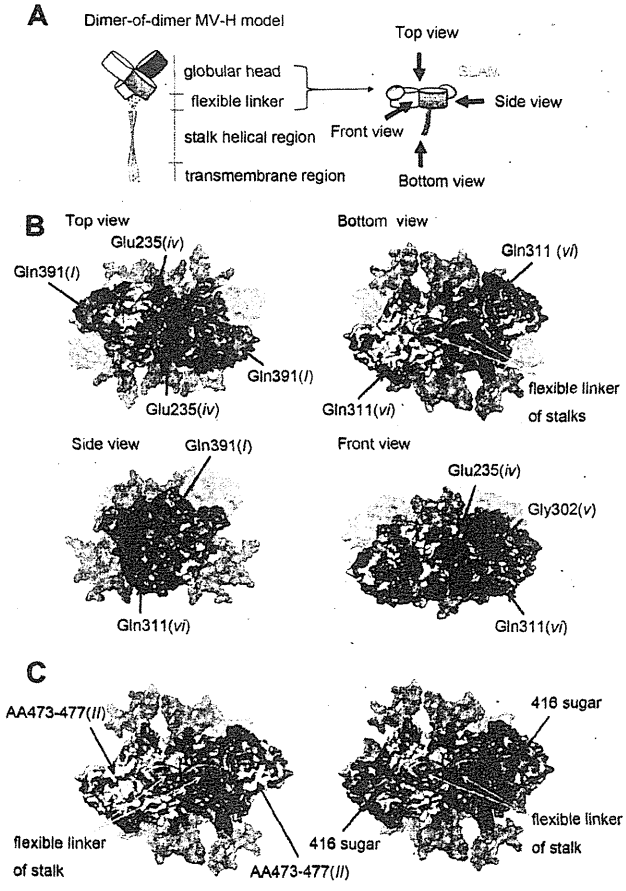

FIG 1 Locations of epitopes on the H protein dimeric structure. (A) Diagrams of a dimer of H protein dimers. The four H protein molecules are shown in gray, light gray, purple, and light purple. SLAM is shown in cyan. (B) Locations of epitopes *I*, *iv*, and *vi*. SLAM and predicted *N*-linked sugars are shown in translucent cyan and magenta, respectively. The amino acid residues demonstrated or suggested to constitute a portion of an epitope are shown in colors: residues on β-sheets 1, 2, 3, 4, 5, and 6 (18) are shown in blue, green, light green, yellow, orange, and red, respectively. (C) Location of epitope *II*. H protein dimers without (left) and with (right) the *N*-linked sugar at position 416 are shown. The figures were produced using PyMOL (Schrödinger; http://www.pymol.org).

TABLE 4 Relation between epitopes and Abs[a]

Epitope name		Region or amino acids which constitute an epitope	Ab which recognizes the epitope	
Present study	Previous papers		Present study	Previous papers
		126–135		MAb48
		185–195		I-44
iv		233–240	E185	BH1
	NE	244–250		BH47, BH59, BH129
v		302	E39	
vi		309–318	E103	I-29, BH38
I	HNE	380–400	E81, B5	BH6, BH21, BH216
		377		BH171
		378		BH168
II		473–477	E128	
		491		16-CD-11
		505–506		80-II-B2
		552		I-41
		587–596		MAb18

[a] Relation between epitopes and Abs in the present and previous studies (10, 41, 42, 47, 51, 53).

from vaccine recipients neutralized all MV strains efficiently, regardless of the glycosylation status at residue 416 (17). Thus, this glycosylation site does not amount to a serious concern with regard to current MV vaccines. However, the additional carbohydrate moiety may provide some advantage for the endemic spread of MV, since the MV strains associated with recent large outbreaks in Europe and Southeast Asia (D4 and D9, respectively) possess this glycosylation site (see Fig. S1 and S2 in the supplemental material) (46). On the other hand, the genotype H1 and D8 strains, which are currently endemic in China and India, respectively, do not have this extra glycosylation site (see Fig. S1 and S2).

Antigenic sites *iv* and *v*, located at the lateral surface of the H protein head dimer, are less important for neutralization. In contrast to genotype D3, MV strains of genotype A were neutralized by E185(*iv*) and E39(*v*) in SLAM$^+$ B95a cells and nectin4$^+$ II-18 cells, respectively (Table 2). We further tested two recombinant MVs possessing chimeric H genes derived from genotypes A and D3 or featuring point mutations [MV323-EGFP-H-β12(N481Y) and MV323-EGFP-H8] (31) for neutralization by E185(*iv*) and E39(*v*) (Fig. 4 and Table 5; see also Table S1 in the supplemental material). The neutralization data demonstrated that amino acids within residues 174 to 334 determined the difference in neutralization by E185(*iv*) and E39(*v*) between MVs with genotypes A and D3. Amino acid substitutions present in this region and predicted to be exposed on the H protein surface (19) were individually introduced into a genotype A virus, resulting in the generation of six additional MVs (Table 6; see also Table S1 in the supplemental material). These recombinant MVs were subjected to neutralization analyses. H protein mutations E235G and G302R rendered the recombinant MVs resistant to neutralization by E185(*iv*) and E39(*v*), respectively (Table 6). These data suggested that residues 235 and 302 are part of epitopes *iv* and *v*, respectively. Epitope *iv* is therefore likely to correspond to the previously reported epitope recognized by BH1 (amino acids 233 to 240 are critical for BH1 binding) (Fig. 5 and Table 4) (47). Both residues are located at the lateral surface of the H protein head dimer, distal from the RBS (Fig. 1B). Furthermore, these epitopes are quite close to the *N*-linked sugars, which may exert some steric hindrance to reduce the binding activities of the Abs (Fig. 1B). These observations are consistent with the weak neutralizing phenotypes of E185(*iv*) and E39(*v*) (Table 2).

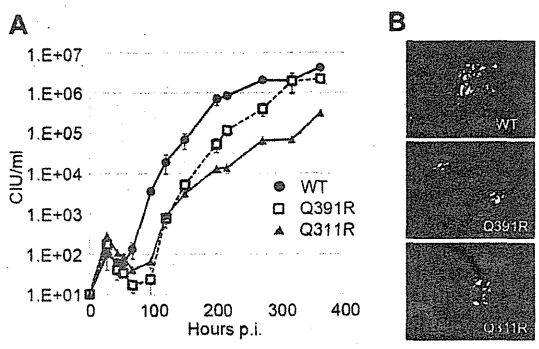

FIG 2 Replication kinetics of two recombinant MVs possessing Q311R or Q391R mutations. (A) Replication kinetics of two escape mutants in II-18 cells. II-18 cells were infected with the MVs at an MOI of 0.01. At various time intervals, cells were harvested in the culture medium and their CIU values were determined in Vero/hSLAM cells. (B) EGFP autofluorescence in MV-infected monolayers of II-18 cells. Panels show representative images obtained with a fluorescence microscope at 6 days postinfection.

Neutralizing Abs that recognize antigenic sites *I* and *II* inhibit receptor binding, while neutralizing Abs specific for antigenic site *vi* interfere with the H-F protein interaction. To mechanistically explore the basis for neutralization by the different MAbs, the effects of the MAbs on the interaction between the H protein (genotype A) and SLAM were analyzed by binding assays using surface plasmon resonance (Biacore assays). MAbs B5(*I*), E81(*I*), and E128(*II*) blocked the binding of the H protein to SLAM, whereas E103(*vi*) did not (Table 7), although all of the MAbs had high neutralization activities (Table 2). These data are consistent with the observations that epitopes *I* and *II* are located near the RBS (10, 45), while epitope *vi* has a more distal position (Fig. 1B). It remains uncertain how epitope *vi* can be a major neutralizing target site. It can be speculated that the epitope may

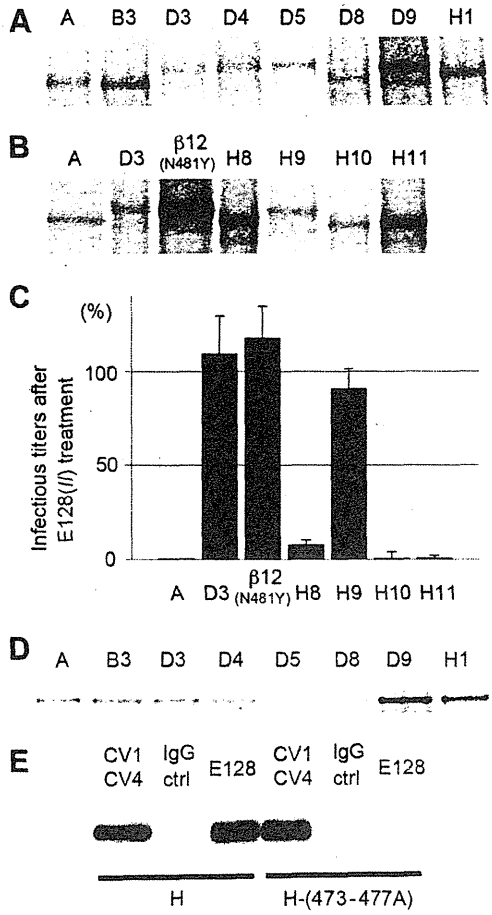

FIG 3 Masking of epitope *II* by the N416-linked sugar. (A) SDS-PAGE analyses for the mobility of H proteins of different genotypes. MV-infected Vero/hSLAM cells at 36 h postinfection were labeled with [^{35}S]methionine-cysteine and lysed in RIPA buffer. Polypeptides were then immunoprecipitated with a polyclonal Ab against MV and resolved by SDS-PAGE. (B) SDS-PAGE analyses for the mobility of H proteins of previously reported recombinant MVs possessing a chimeric H gene between the IC323 (genotype D3) and Edmonston (genotype A) strains or various point mutations. (C) Neutralizing assays of E128 against EGFP-expressing MV strains possessing a chimeric H gene between the IC323 (genotype D3) and Edmonston (genotype A) strains or various point mutations. The CIU of each virus was determined in II-18 cells in the presence or absence of E128. The CIU determined in the presence of E128 was compared with that in the absence of E128. The CIU in the absence of E128 was set to 100%. (D) SDS-PAGE analyses for the mobility of Endo-H-treated H proteins of different genotypes. (E) A five-residue alanine substitution in the H protein at residues 473 to 477 prevents binding of MAb E128. Immunoprecipitation of MV H_{Flag} and CD46-binding defective MV H_{Flag}-(473-477A) with MAbs CV1/CV4 and E128. The immunoprecipitated material was gel fractionated, followed by immunoblotting and detection of H_{Flag} with an anti-Flag M2 antibody. IgG ctrl; control IgG.

TABLE 5 Amino acid differences in recombinant MVs

Amino acid position	Amino acid difference in recombinant MV[a]: A	D3	β12(N481Y)	H8	H9	H10	H11
174	T	A	T	A	A	A	A
176	T	A	T	A	A	A	A
211	G	S	G	S	S	S	S
235	E	G	E	G	G	G	G
243	K	G	K	G	G	G	G
252	Y	H	Y	H	H	H	H
276	L	F	L	F	F	F	F
284	L	F	L	F	F	F	F
296	L	F	L	F	F	F	F
302	G	R	G	R	R	R	R
334	Q	R	Q	R	R	R	R
390	I	N	N	I	I	N	I
416	D	N	N	D	N	D	D
446	S	T	T	T	S	S	S
481	Y	N	Y	Y	Y	Y	Y
492	G	E	E	G	G	G	E
575	Q	K	K	K	K	K	K

[a] These recombinant MVs were reported previously (31).

be involved in one or some of the fusion steps other than the receptor binding. To examine whether the H-F protein interaction affects MAb binding, coimmunoprecipitation of MV envelope glycoprotein complexes was performed (36). Compared with a reference Ab cocktail, the amount of F protein coimmunoprecipitated with H protein was reduced by ~50% when E103(*vi*) was used (Fig. 6). These data suggested that epitope *vi* is influenced by the H-F protein interaction. Interestingly, the higher order (tetrameric) structures of the H protein-SLAM complex proposed on the basis of the crystal structures suggest that epitope *vi* in two of the four H molecules (gray and light purple H molecules) is located at the bottom surface proximal to the stalk region, while that in the other two molecules (light gray and purple H molecules) forms part of the interface of the H protein dimers in form I, one of the tetrameric structures (Fig. 7A) (18), but not form II, the other tetrameric structure (Fig. 7B) (18). Furthermore, epitope *vi* appears to contact epitope *iv* at the interface (Fig. 7A). Epitope *iv* corresponds to the BH1-binding epitope (Table 4) (47), and most likely forms a single epitope together with a previously reported linear neutralizing epitope (NE) (amino acid positions 244 to 250) (Table 4) (47), although a definitive conclusion could not be made, because eight amino acids (positions 240 to 247) were so flexible that little electron density was observed in the H crystal structures (Fig. 5) (18).

DISCUSSION

In the present study, we focused on neutralizing Abs directed against the H protein, because the protective immunity is predominantly humoral (48) and H protein-specific Abs mainly account for the neutralization activity in serum from vaccinated

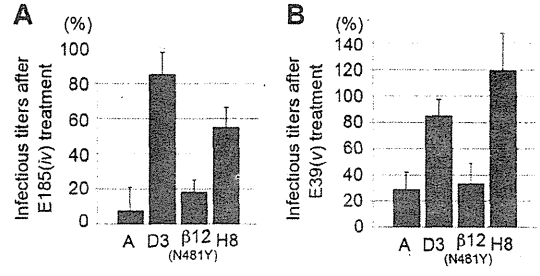

FIG 4 Neutralizing assays of E185 and E39 against EGFP-expressing MV strains with different H protein sequences. (A) The CIU of each virus was determined in B95a cells in the presence or absence of E185. (B) The CIU of each virus was determined in II-18 cells in the presence or absence of E39. The CIU determined in the presence of the Abs was compared with that in the absence of the Abs. The CIU in the absence of the Abs was set to 100%.

TABLE 6 Neutralizing titers against recombinant MV possessing the Edmonston H protein with various amino acid substitutions[a]

Mutation	Neutralizing titer against recombinant MV: E185(*iv*) in B95a	E39(*v*) in II-18
(−)	494	1,750
G211S	494	875
E235G	62	1,750
Y252H	494	1,750
L284F	494	1,750
L296F	494	1,750
G302R	494	<27

[a] Neutralizing titers for 1 mg/ml of Ig. (−), parental virus.

individuals (9–11). A key finding in the present study is that the antigenic site *vi*, which is unrelated to receptor binding but probably involved in the formation of a higher-order H-F protein oligomeric structure (34, 36, 49), is a major neutralizing epitope that is conserved among different genotype strains. This type of epitopes has been predicted by previous studies, although receptor binding has been tested for CD46, but not the wild-type receptors, SLAM, or nectin4 (10, 47, 50). One of them, known as NE, is recognized by BH47, BH59, and BH129 MAbs (Table 4) (10, 47). The other is recognized by I-29 (10, 50) and was determined as the epitope *vi* in the present study (Table 4). Therefore, our data are consistent with the previous studies that MAbs that recognize the epitope *vi* neutralize MV infection by inhibiting virus fusion without affecting the receptor binding (10, 50). Membrane fusion of MV is mediated by concerted actions of the H and F proteins. Binding of the H protein to a receptor triggers F protein-mediated membrane fusion. Although the triggering mechanism remains largely unknown, accumulated data indicate that rearrangement of an H-F protein oligomeric structure is a key for triggering fusion (18, 34, 36, 49). This epitope is fully conserved among different MV genotypes. A requirement for the formation of a functional fusion complex is likely to generate structural constraints that prevent substitutions in this epitope.

We also found that a large area containing epitopes *I* and *II* serves as a target for the humoral anti-MV response. Our data showed that MAbs B5 and E81 bind to an epitope (epitope *I*) corresponding to a previously reported hemagglutination and neutralization epitope (HNE) (amino acid positions 380 to 400), which is recognized by MAbs BH6, BH21, and BH216 (Table 4 and Fig. 8) (10, 41, 51). Six residues (positions 386, 387, 388, 391, 394, and 395) were shown to be critical for Ab binding (52). Accordingly, a Q391R substitution was sufficient for MV escape from neutralization by B5 and E81. On the other hand, epitope *II* maps to residues 473 to 477, which are located at the bottom surface of the H protein head domain and involved in interaction with CD46 (10, 45). In some of the current wild-type MV strains,

TYLVEKPNLSSKRSELSQLSMY
AA233-240: BH1-binding site AA244-250: NE

TYLVEKPNL--------QLSMY

FIG 5 Amino acid sequence of epitope *iv*. The amino acid residues at positions 231 to 252 are shown. The residues known to constitute part of the epitope are shown in blue characters (top). The amino acid residues represented in the crystal structures are shown. Missing residues are indicated by dashes.

TABLE 7 Competitive binding of anti-H protein MAbs against SLAM

Ab	Antigenic site	Competitive activity[a]
B5	*I*	++
E81	*I*	+
E128	*II*	++
E103	*vi*	−

[a] ++, Complete inhibition; +, weak inhibition; −, no inhibition.

this epitope is masked by an additional carbohydrate moiety (Asn416). Previous studies revealed that MV escape from MAb 16-CD-11 can be achieved through an amino acid substitution at position 491 in the H protein (41) and that escape mutants from MAbs BH171 and BH168 possess substitutions at positions 377 and 378, respectively (Table 4) (10, 53). The residues at positions 491, 377, and 378 in the H protein are located between the HNE (epitope *I*) and epitope *II* (Table 4 and Fig. 8). It was further shown that H protein binding of MAbs BH30 and BH99 competes with 16-CD-11 (10, 41). Taken together, these data support that a large area of the H protein head domain spanning from epitope *I* to epitope *II* can serve as a target for neutralizing Abs (Fig. 8). Our data suggest that the region around epitope *I* has structural con-

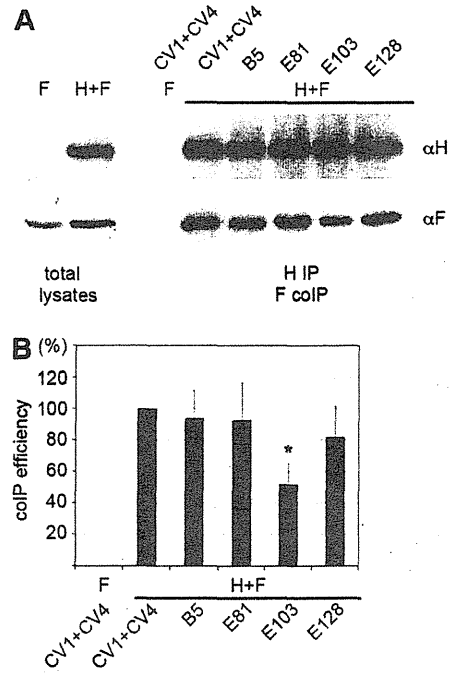

FIG 6 MV H and F protein coimmunoprecipitation. MAb E103 shows reduced immunoprecipitation efficiency for H/F hetero-oligomers. (A) Vero cells transiently transfected with expression plasmids encoding MV H_{Flag} and F_{HA}, or F_{HA} only as a control, were immunoprecipitated with specific MAbs directed against the MV H protein ectodomain (CV1/CV4, B5, E81, E103, or E128 as indicated). Precipitated H_{Flag} material was labeled with an anti-Flag M2 antibody, and the coprecipitated F_{HA} was detected with an anti-HA 16b12 antibody. (B) For densitometric quantification, the ratio of F_{HA} to H_{Flag} signals was determined for each MAb, followed by normalization to the coimmunoprecipitation ratio obtained with the CV1/CV4 reference MAb mixture. Data represent the means ± standard errors of the means (SEM) of results from three experiments. The asterisk indicates that, in F densitometry, a *t* test returned *P* values of <0.05 for the difference in coimmunoprecipitation (CoIP) efficiency, with E103 relative to the CV1+CV4 reference.

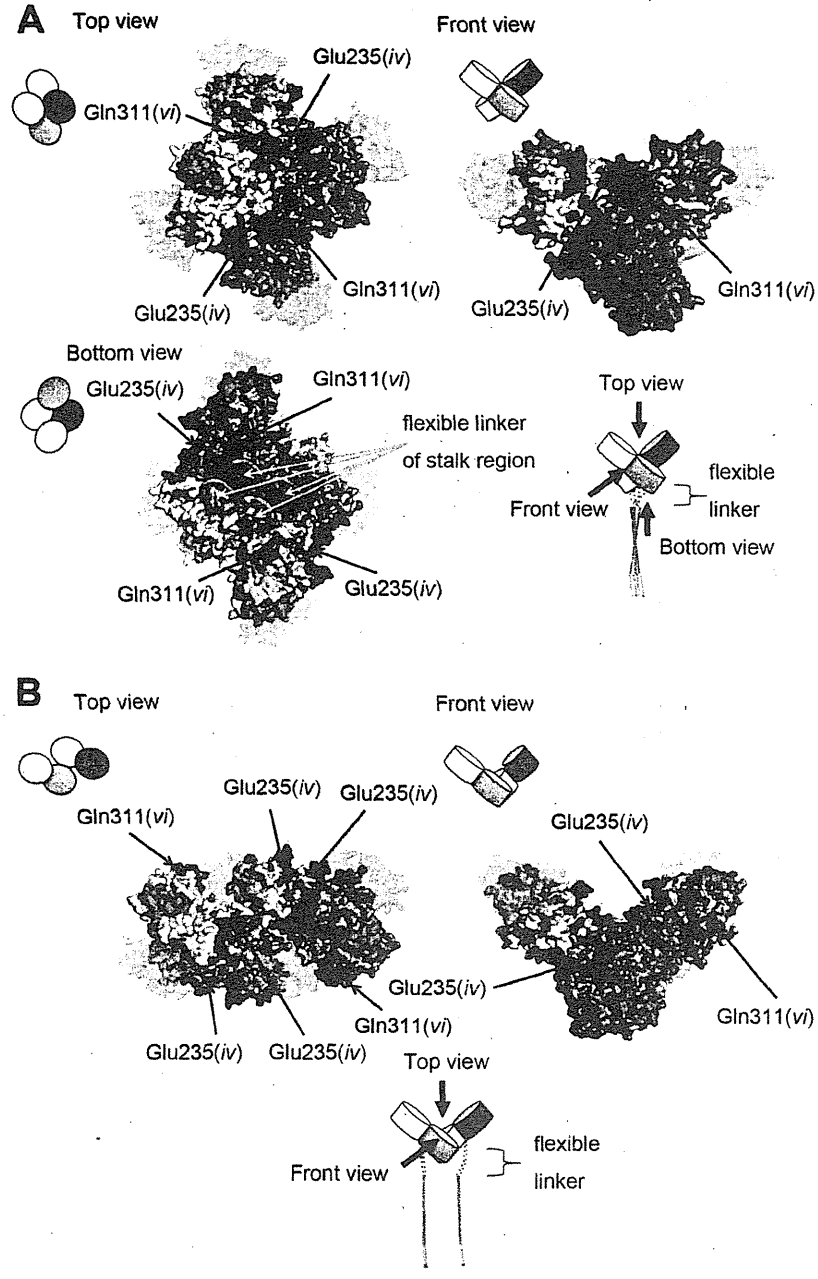

FIG 7 Locations of epitopes *iv* and *vi* on the H protein tetrameric structure. The four H protein molecules are shown in gray, light gray, purple, and light purple. SLAM is shown in translucent cyan. The amino acid residues demonstrated or suggested to constitute a portion of an epitope are shown in colors: residues on β-sheets 1, 2, 3, 4, 5, and 6 (18) are shown in blue, green, light green, yellow, orange, and red, respectively. (A) A tetrameric structure in form I (18). (B) A tetrameric structure in form II (18).

straints for change, since it is conserved among different genotype strains, thereby contributing to the single serotype nature of MV.

In summary, the H protein of MV possesses at least two conserved effective neutralizing epitopes. One, which is a previously recognized HNE epitope, is located near the RBS, and thus MAbs that recognize this epitope blocked the receptor binding of the H protein. On the other hand, the other epitope is located at the position distant from the RBS. Thus, MAbs that recognizes this epitope did not inhibit the receptor binding of the H protein but rather interfered with the H-F interaction. Based on the structural data of MV H protein, it was predicted that, when the H protein forms a tetramer, this epitope locates at two positions: the contact face of two H protein dimers and the bottom face of the head of the H protein tetramer. This epitope possibly plays a key role in the formation of a higher-order H-F protein oligomeric structure. Our data also demonstrated that one effective neutralizing epitope is not conserved, since the epitope has been masked by an *N*-linked sugar modification in some genotype MV strains. The data in the

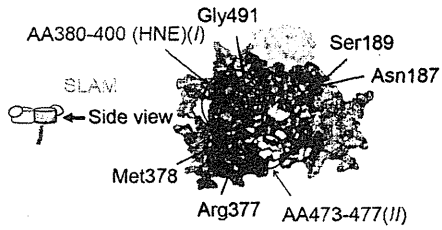

FIG 8 A major epitope region covering a large area containing epitopes *I* and *II*. A side view of a dimer is shown. SLAM and predicted sugars are shown in translucent cyan and magenta, respectively. The amino acid residues demonstrated or suggested to constitute a portion of an epitope are shown in colors: residues on β-sheet 1, 2, 3, 4, 5, and 6 (18) are shown in blue, green, light green, yellow, orange, and red, respectively.

present study contribute to our understanding of the antigenicity of MV and support the global elimination program of measles.

ACKNOWLEDGMENTS

We thank T.A. Sato and T. Seya for providing MAbs, N. Ito and M. Sugiyama for providing the BHK/T7-9 cells, and K. Taira for providing an MV isolate. We also thank Y. Yanagi for invaluable suggestions and providing useful cell lines and all the members of the Department of Virology 3, NIID, Japan, for technical support.

This work was supported in part by grants from the Ministry of Education, Culture, Sports, Science and Technology and the Ministry of Health, Labor and Welfare of Japan and by a grant from The Takeda Science Foundation (to M.T.). The work of M.A.B. and R.K.P. was supported in part by Public Health Service grant AI083402 from the NIH/NIAID (to R.K.P.).

REFERENCES

1. Bryce J, Boschi-Pinto C, Shibuya K, Black RE. 2005. WHO estimates of the causes of death in children. Lancet 365:1147–1152.
2. Strebel PM, Cochi SL, Hoekstra E, Rota PA, Featherstone D, Bellini WJ, Katz SL. 2011. A world without measles. J. Infect. Dis. 204(Suppl 1):S1–S3.
3. Sanders R, Dabbagh A, Featherstone D. 2011. Risk analysis for measles reintroduction after global certification of eradication. J. Infect. Dis. 204(Suppl 1):S71–S77.
4. Bellini WJ, a Rota PA. 2011. Biological feasibility of measles eradication. Virus Res. 162:72–79.
5. Tatsuo H, Ono N, Tanaka K, Yanagi Y. 2000. SLAM (CDw150) is a cellular receptor for measles virus. Nature 406:893–897.
6. Noyce RS, Bondre DG, Ha MN, Lin LT, Sisson G, Tsao MS, Richardson CD. 2011. Tumor cell marker PVRL4 (nectin 4) is an epithelial cell receptor for measles virus. PLoS Pathog. 7:e1002240. doi:10.1371/journal.ppat.1002240.
7. Muhlebach MD, Mateo M, Sinn PL, Prufer S, Uhlig KM, Leonard VH, Navaratnarajah CK, Frenzke M, Wong XX, Sawatsky B, Ramachandran S, McCray PB, Jr, Cichutek K, von Messling V, Lopez M, Cattaneo R. 2011. Adherens junction protein nectin-4 is the epithelial receptor for measles virus. Nature 480:530–533.
8. Takeda M, Tahara M, Nagata N, Seki F. 2011. Wild-type measles virus is intrinsically dual-tropic. Front. Microbiol. 2:279.
9. de Swart RL, Yuksel S, Osterhaus AD. 2005. Relative contributions of measles virus hemagglutinin- and fusion protein-specific serum antibodies to virus neutralization. J. Virol. 79:11547–11551.
10. Bouche FB, Ertl OT, Muller CP. 2002. Neutralizing B cell response in measles. Viral Immunol. 15:451–471.
11. de Swart RL, Yuksel S, Langerijs CN, Muller CP, Osterhaus AD. 2009. Depletion of measles virus glycoprotein-specific antibodies from human sera reveals genotype-specific neutralizing antibodies. J. Gen. Virol. 90: 2982–2989.
12. WHO. 2012. Measles virus nomenclature update: 2012. Wkly. Epidemiol. Rec. 87:73–81.
13. Finsterbusch T, Wolbert A, Deitemeier I, Meyer K, Mosquera MM, Mankertz A, Santibanez S. 2009. Measles viruses of genotype H1 evade recognition by vaccine-induced neutralizing antibodies targeting the linear haemagglutinin noose epitope. J. Gen. Virol. 90:2739–2745.
14. Shi J, Zheng J, Huang H, Hu Y, Bian J, Xu D, Li F. 2011. Measles incidence rate and a phylogenetic study of contemporary genotype H1 measles strains in China: is an improved measles vaccine needed? Virus Genes 43:319–326.
15. Tamin A, Rota PA, Wang ZD, Heath JL, Anderson LJ, Bellini WJ. 1994. Antigenic analysis of current wild type and vaccine strains of measles virus. J. Infect. Dis. 170:795–801.
16. Kuhne M, Brown DW, Jin L. 2006. Genetic variability of measles virus in acute and persistent infections. Infect. Genet. Evol. 6:269–276.
17. Santibanez S, Niewiesk S, Heider A, Schneider-Schaulies J, Berbers GA, Zimmermann A, Halenius A, Wolbert A, Deitemeier I, Tischer A, Hebgek H. 2005. Probing neutralizing-antibody responses against emerging measles viruses (MVs): immune selection of MV by H protein-specific antibodies? J. Gen. Virol. 86:365–374.
18. Hashiguchi T, Ose T, Kubota M, Maita N, Kamishikiryo J, Maenaka K, Yanagi Y. 2011. Structure of the measles virus hemagglutinin bound to its cellular receptor SLAM. Nat. Struct. Mol. Biol. 18:135–141.
19. Hashiguchi T, Kajikawa M, Maita N, Takeda M, Kuroki K, Sasaki K, Kohda D, Yanagi Y, Maenaka K. 2007. Crystal structure of measles virus hemagglutinin provides insight into effective vaccines. Proc. Natl. Acad. Sci. U. S. A. 104:19535–19540.
20. Shirogane Y, Takeda M, Tahara M, Ikegame S, Nakamura T, Yanagi Y. 2010. Epithelial-mesenchymal transition abolishes the susceptibility of polarized epithelial cell lines to measles virus. J. Biol. Chem. 285:20882–20890.
21. Kobune F, Sakata H, Sugiura A. 1990. Marmoset lymphoblastoid cells as a sensitive host for isolation of measles virus. J. Virol. 64:700–705.
22. Ito N, Takayama-Ito M, Yamada K, Hosokawa J, Sugiyama M, Minamoto N. 2003. Improved recovery of rabies virus from cloned cDNA using a vaccinia virus-free reverse genetics system. Microbiol. Immunol. 47:613–617.
23. Ono N, Tatsuo H, Hidaka Y, Aoki T, Minagawa H, Yanagi Y. 2001. Measles viruses on throat swabs from measles patients use signaling lymphocytic activation molecule (CDw150) but not CD46 as a cellular receptor. J. Virol. 75:4399–4401.
24. Takeda M, Tahara M, Hashiguchi T, Sato TA, Jinnouchi F, Ueki S, Ohno S, Yanagi Y. 2007. A human lung carcinoma cell line supports efficient measles virus growth and syncytium formation via a SLAM- and CD46-independent mechanism. J. Virol. 81:12091–12096.
25. Sato TA, Fukuda A, Sugiura A. 1985. Characterization of major structural proteins of measles virus with monoclonal antibodies. J. Gen. Virol. 66(Pt 7):1397–1409.
26. Sato TA, Enami M, Kohama T. 1995. Isolation of the measles virus hemagglutinin protein in a soluble form by protease digestion. J. Virol. 69:513–516.
27. Sakata H, Hishiyama M, Sugiura A. 1984. Enzyme-linked immunosorbent assay compared with neutralization tests for evaluation of live mumps vaccines. J. Clin. Microbiol. 19:21–25.
28. Takeda M, Takeuchi K, Miyajima N, Kobune F, Ami Y, Nagata N, Suzaki Y, Nagai Y, Tashiro M. 2000. Recovery of pathogenic measles virus from cloned cDNA. J. Virol. 74:6643–6647.
29. Radecke F, Spielhofer P, Schneider H, Kaelin K, Huber M, Dotsch C, Christiansen G, Billeter MA. 1995. Rescue of measles viruses from cloned DNA. EMBO J. 14:5773–5784.
30. Hashimoto K, Ono N, Tatsuo H, Minagawa H, Takeda M, Takeuchi K, Yanagi Y. 2002. SLAM (CD150)-independent measles virus entry as revealed by recombinant virus expressing green fluorescent protein. J. Virol. 76:6743–6749.
31. Tahara M, Takeda M, Seki F, Hashiguchi T, Yanagi Y. 2007. Multiple amino acid substitutions in hemagglutinin are necessary for wild-type measles virus to acquire the ability to use receptor CD46 efficiently. J. Virol. 81:2564–2572.
32. Tahara M, Takeda M, Shirogane Y, Hashiguchi T, Ohno S, Yanagi Y. 2008. Measles virus infects both polarized epithelial and immune cells by using distinctive receptor-binding sites on its hemagglutinin. J. Virol. 82: 4630–4637.
33. Seki F, Yamada K, Nakatsu Y, Okamura K, Yanagi Y, Nakayama T, Komase K, Takeda M. 2011. The SI strain of measles virus derived from a patient with subacute sclerosing panencephalitis possesses typical genome alterations and unique amino acid changes that modulate receptor specificity and reduce membrane fusion activity. J. Virol. 85:11871–11882.

34. Brindley MA, Plemper RK. 2010. Blue native PAGE and biomolecular complementation reveal a tetrameric or higher-order oligomer organization of the physiological measles virus attachment protein H. J. Virol. 84:12174–12184.
35. Plemper RK, Hammond AL, Gerlier D, Fielding AK, Cattaneo R. 2002. Strength of envelope protein interaction modulates cytopathicity of measles virus. J. Virol. 76:5051–5061.
36. Paal T, Brindley MA, St Clair C, Prussia A, Gaus D, Krumm SA, Snyder JP, Plemper RK. 2009. Probing the spatial organization of measles virus fusion complexes. J. Virol. 83:10480–10493.
37. Corey EA, Iorio RM. 2009. Measles virus attachment proteins with impaired ability to bind CD46 interact more efficiently with the homologous fusion protein. Virology 383:1–5.
38. Tahara M, Takeda M, Yanagi Y. 2005. Contributions of matrix and large protein genes of the measles virus Edmonston strain to growth in cultured cells as revealed by recombinant viruses. J. Virol. 79:15218–15225.
39. Takeda M, Ohno S, Tahara M, Takeuchi H, Shirogane Y, Ohmura H, Nakamura T, Yanagi Y. 2008. Measles viruses possessing the polymerase protein genes of the Edmonston vaccine strain exhibit attenuated gene expression and growth in cultured cells and SLAM knock-in mice. J. Virol. 82:11979–11984.
40. Leonard VH, Sinn PL, Hodge G, Miest T, Devaux P, Oezguen N, Braun W, McCray PB, McChesney MB, Cattaneo R. 2008. Measles virus blind to its epithelial cell receptor remains virulent in rhesus monkeys but cannot cross the airway epithelium and is not shed. J. Clin. Invest. 118:2448–2458.
41. Ertl OT, Wenz DC, Bouche FB, Berbers GA, Muller CP. 2003. Immunodominant domains of the Measles virus hemagglutinin protein eliciting a neutralizing human B cell response. Arch. Virol. 148:2195–2206.
42. Hu A, Sheshberadaran H, Norrby E, Kovamees J. 1993. Molecular characterization of epitopes on the measles virus hemagglutinin protein. Virology 192:351–354.
43. Rota JS, Hummel KB, Rota PA, Bellini WJ. 1992. Genetic variability of the glycoprotein genes of current wild-type measles isolates. Virology 188: 135–142.
44. Sakata H, Kobune F, Sato TA, Tanabayashi K, Yamada A, Sugiura A. 1993. Variation in field isolates of measles virus during an 8-year period in Japan. Microbiol. Immunol. 37:233–237.
45. Patterson JB, Scheiflinger F, Manchester M, Yilma T, Oldstone MB. 1999. Structural and functional studies of the measles virus hemagglutinin: identification of a novel site required for CD46 interaction. Virology 256:142–151.
46. Rota PA, Brown K, Mankertz A, Santibanez S, Shulga S, Muller CP, Hubschen JM, Siqueira M, Beirnes J, Ahmed H, Triki H, Al-Busaidy S, Dosseh A, Byabamazima C, Smit S, Akoua-Koffi C, Bwogi J, Bukenya H, Wairagkar N, Ramamurty N, Incomserb P, Pattamadilok S, Jee Y, Lim W, Xu W, Komase K, Takeda M, Tran T, Castillo-Solorzano C, Chenoweth P, Brown D, Mulders MN, Bellini WJ, Featherstone D. 2011. Global distribution of measles genotypes and measles molecular epidemiology. J. Infect. Dis. 204(Suppl 1):S514–S523.
47. Fournier P, Brons NH, Berbers GA, Wiesmuller KH, Fleckenstein BT, Schneider F, Jung G, Muller CP. 1997. Antibodies to a new linear site at the topographical or functional interface between the haemagglutinin and fusion proteins protect against measles encephalitis. J. Gen. Virol. 78(Pt 6):1295–1302.
48. Duke T, Mgone CS. 2003. Measles: not just another viral exanthem. Lancet 361:763–773.
49. Ader N, Brindley MA, Avila M, Origgi FC, Langedijk JP, Orvell C, Vandevelde M, Zurbriggen A, Plemper RK, Plattet P. 2012. Structural rearrangements of the central region of the morbillivirus attachment protein stalk domain trigger F protein refolding for membrane fusion. J. Biol. Chem. 287:16324–16334.
50. Makela MJ, Salmi AA, Norrby E, Wild TF. 1989. Monoclonal antibodies against measles virus haemagglutinin react with synthetic peptides. Scand. J. Immunol. 30:225–231.
51. Ziegler D, Fournier P, Berbers GA, Steuer H, Wiesmuller KH, Fleckenstein B, Schneider F, Jung G, King CC, Muller CP. 1996. Protection against measles virus encephalitis by monoclonal antibodies binding to a cystine loop domain of the H protein mimicked by peptides which are not recognized by maternal antibodies. J. Gen. Virol. 77(Pt 10):2479–2489.
52. Putz MM, Hoebeke J, Ammerlaan W, Schneider S, Muller CP. 2003. Functional fine-mapping and molecular modeling of a conserved loop epitope of the measles virus hemagglutinin protein. Eur. J. Biochem. 270: 1515–1527.
53. Liebert UG, Flanagan SG, Loffler S, Baczko K, ter Meulen V, Rima BK. 1994. Antigenic determinants of measles virus hemagglutinin associated with neurovirulence. J. Virol. 68:1486–1493.

Journal of Virology

Lethal Canine Distemper Virus Outbreak in Cynomolgus Monkeys in Japan in 2008

Kouji Sakai, Noriyo Nagata, Yasushi Ami, Fumio Seki, Yuriko Suzaki, Naoko Iwata-Yoshikawa, Tadaki Suzuki, Shuetsu Fukushi, Tetsuya Mizutani, Tomoki Yoshikawa, Noriyuki Otsuki, Ichiro Kurane, Katsuhiro Komase, Ryoji Yamaguchi, Hideki Hasegawa, Masayuki Saijo, Makoto Takeda and Shigeru Morikawa

J. Virol. **2013, 87(2):1105. DOI: 10.1128/JVI.02419-12.**
Published Ahead of Print 7 November 2012.

JVI
Journals.ASM.org

Lethal Canine Distemper Virus Outbreak in Cynomolgus Monkeys in Japan in 2008

Kouji Sakai,[a] Noriyo Nagata,[b] Yasushi Ami,[c] Fumio Seki,[a] Yuriko Suzaki,[c] Naoko Iwata-Yoshikawa,[b] Tadaki Suzuki,[b] Shuetsu Fukushi,[d] Tetsuya Mizutani,[d] Tomoki Yoshikawa,[d] Noriyuki Otsuki,[a] Ichiro Kurane,[d] Katsuhiro Komase,[a] Ryoji Yamaguchi,[f] Hideki Hasegawa,[b] Masayuki Saijo,[d] Makoto Takeda,[a] Shigeru Morikawa[d,e]

Department of Virology III,[a] Department of Pathology,[b] Division of Experimental Animal Research,[c] Department of Virology I,[d] Department of Veterinary Science,[e] National Institute of Infectious Diseases, Tokyo, Japan; Department of Veterinary Pathology, Faculty of Agriculture, University of Miyazaki, Miyazaki, Japan[f]

Canine distemper virus (CDV) has recently expanded its host range to nonhuman primates. A large CDV outbreak occurred in rhesus monkeys at a breeding farm in Guangxi Province, China, in 2006, followed by another outbreak in rhesus monkeys at an animal center in Beijing in 2008. In 2008 in Japan, a CDV outbreak also occurred in cynomolgus monkeys imported from China. In that outbreak, 46 monkeys died from severe pneumonia during a quarantine period. A CDV strain (CYN07-dV) was isolated in Vero cells expressing dog signaling lymphocyte activation molecule (SLAM). Phylogenic analysis showed that CYN07-dV was closely related to the recent CDV outbreaks in China, suggesting continuing chains of CDV infection in monkeys. *In vitro*, CYN07-dV uses macaca SLAM and macaca nectin4 as receptors as efficiently as dog SLAM and dog nectin4, respectively. CYN07-dV showed high virulence in experimentally infected cynomolgus monkeys and excreted progeny viruses in oral fluid and feces. These data revealed that some of the CDV strains, like CYN07-dV, have the potential to cause acute systemic infection in monkeys.

Canine distemper virus (CDV) causes acute systemic infection in dogs and other Canidae, with symptoms of fever, coughing, vomiting, diarrhea, ataxia, and paralysis. It has long been thought that only animals in the family Canidae are susceptible to CDV infection in nature. However, during the last 2 decades, animals of many other species, such as Ailuridae (1), Mustelidae (2), Viverridae (3, 4), Procyonidae (5), Phocidae (6), and Felidae (7, 8), have been infected with CDV in nature.

CDV belongs to the genus *Morbillivirus* within the family Paramyxoviridae (9). Signaling lymphocyte activation molecule (SLAM) is a principal receptor of CDV. Other members of the *Morbillivirus* genus, namely, measles virus (MV), rinderpest virus, and peste des petits ruminants virus, are also known to utilize human, bovine, and goat SLAM, respectively, as a receptor. These viruses preferentially use the SLAM of their host animals but have the ability to use other SLAMs of nonhost animals with reduced efficiency (10). Recently, human nectin4 and dog nectin4 have been identified as epithelial cell receptors for MV (11, 12) and CDV (13), respectively.

Importantly, CDV outbreaks have recently emerged with a high mortality rate in nonhuman primates. The first outbreak occurred in 1989 in Japan (14). Twenty-two Japanese monkeys (*Macaca fuscata*) in the wild were captured and later shown to have CDV infections. Two of them developed neurological symptoms, and one died of encephalitis (14). Recently, large CDV outbreaks have occurred in rhesus monkeys (*Macaca mulatta*) at a breeding farm in Guangxi province, China, with a mortality rate of 5 to 30% (15). In 2008, an animal center in Beijing, China, experienced another CDV outbreak in rhesus monkeys (16). This outbreak was likely associated with the Guangxi outbreaks. Following these outbreaks in China, a CDV outbreak occurred in cynomolgus monkeys (*Macaca fascicularis*) in Japan in 2008. These monkeys were imported from China, and some 46 cynomolgus monkeys out of 432 imported were euthanized or died from severe pneumonia, diarrhea, and anorexia during a quarantine period. A CDV strain was isolated from a moribund monkey, and phylogenic analysis of its genome sequence showed that the CDV strain was closely related to the CDV strains associated with recent outbreaks in rhesus monkeys in China, suggesting continuing chains of CDV infection in monkeys. In the present study, we analyzed the pathogenicity of the CDV strain in cynomolgus monkeys. We also investigated whether the CDV strain utilized macaca SLAM and macaca nectin4 as its receptors.

MATERIALS AND METHODS

Cells. Vero cells constitutively expressing dog SLAM (Vero.DogSLAMtag) and dog nectin4 (Vero/dNectin4) were used (13, 17). Vero cells expressing human SLAM (Vero/hSLAM) (10) were also used. Vero cells constitutively expressing macaca SLAM (Vero/macSLAM) and macaca nectin4 (Vero/macNectin4) were generated in the present study. Total RNAs obtained from peripheral blood mononuclear cells (PBMCs) and a kidney from a cynomolgus monkey were used to synthesize cDNAs of macaca SLAM and macaca nectin4, respectively. The nucleotide sequences of cynomolgus SLAM and cynomolgus nectin4 were deposited in GenBank with accession numbers AB742520 and AB742522, respectively. The macaca SLAM and macaca nectin4 cDNA fragments were inserted into the pCXN2 vector (18), generating pCXN2-macSLAM and pCXN2-macNectin4, respectively. Vero/macSLAM and Vero/macNectin4 cells were generated by transfecting Vero cells with pCXN2-macSLAM and pCXN2-macNectin4, respectively, and were selected in Dulbecco's modified Eagle's medium (DMEM) supplemented with 7% fetal bovine serum (FBS) and 0.5 mg/ml Geneticin (G418; Invitrogen). Expression of macaca SLAM and nectin4 in Vero cells was confirmed by immunofluorescence

Received 5 September 2012 Accepted 1 November 2012
Published ahead of print 7 November 2012
Address correspondence to Shigeru Morikawa, morikawa@nih.go.jp.

doi:10.1128/JVI.02419-12

staining using a goat anti-human SLAM and nectin4 polyclonal antibody, respectively.

Virus isolation. Tissue samples obtained from the spleens of moribund or dead monkeys were suspended in phosphate-buffered saline (PBS) supplemented with antibiotics and were homogenized. The homogenates were centrifuged at 10,000 × *g* for 5 min, and supernatants were inoculated to monolayers of Vero.DogSLAMtag cells.

RNA extraction and RT-PCR. Viral and total RNAs were extracted from culture media and cells, respectively, using ISOGEN-LS (Nippon Gene). Reverse transcription (RT) was carried out with Superscript III (Invitrogen) using primers of random nucleotide hexamers (TaKaRa Bio Inc.). Then, PCR was performed to amplify CDV-specific cDNA fragments.

Sequencing and phylogenic analysis of the CDV isolate. PCR amplicons were used as templates for sequencing on an Applied Biosystems 3130 automated DNA sequencer using a BigDye Terminator version 3.1 cycle sequencing kit (Applied Biosystems Japan). The entire genome nucleotide sequence was determined using overlapping PCR amplicons. The nucleotide sequence of each extremity was determined by the rapid amplification of cDNA ends (RACE) method. The sequence was further confirmed by using a Roche GS Junior sequencer. Nucleotide and amino acid sequence identities were calculated using the pairwise distance algorithm (*p* distance) with MEGA 4 software (19). Phylograms were reconstructed using a neighbor-joining algorithm with MEGA 4 software. The robustness of the resulting branching patterns was tested using the bootstrap method with 1,000 replicates. Sequence relatedness is shown as percentage identity.

Histopathological examination of monkeys infected with CDV during the 2008 outbreak. Three cynomolgus monkeys (11, 12, and 13) infected with CDV during the 2008 outbreak were euthanized by exsanguination under excess ketamine anesthesia and autopsied for histopathological examination. Tissue samples were immersed in 10% phosphate-buffered formalin. Fixed tissues were embedded in paraffin, sectioned, and stained with hematoxylin and eosin. Immunohistochemical analysis for the detection of the CDV antigens was performed on paraffin-embedded sections using EnVison/HRP Systems (Dako). After deparaffinization with xylene, the sections were rehydrated in ethanol and immersed in PBS. Antigens were retrieved by hydrolytic autoclaving for 15 min at 121°C in a sodium citrate-sodium chloride buffer (10 mM, pH 6.0). Endogenous peroxidase was blocked by incubation in 1% hydrogen peroxide in methanol for 30 min. The sections were incubated with a monoclonal antibody against CDV nucleoprotein (NP) (VMRD Inc.) and then with biotin-conjugated anti-mouse IgG. Peroxidase activity was detected by development with diaminobenzidine containing hydrogen peroxide, and then the nuclei were counterstained by hematoxylin.

Double immunofluorescence stainings were also performed for the various tissues of the CDV-infected cynomolgus monkey 11. Rabbit anti-wide-spectrum cytokeratin antibody (ab9377; Abcam), rabbit anti-neuron-specific β III tubulin antibody (ab56110; Abcam), rabbit anti-CD3 antibody [SP7] (ab21703; Abcam), goat anti-nectin4 polyclonal antibody (R&D Systems), and the monoclonal antibody against CDV NP were used as primary antibodies. Normal rabbit, goat, and mouse sera were used as negative-control antibodies (Dako). The sections were deparaffinized, rehydrated, and immersed in PBS. Antigens were retrieved by hydrolytic autoclaving in the retrieval solution (pH 9.0; Nichirei) for 15 min at 121°C. After the sections were cooled, to block background staining, normal goat or donkey sera were used. The sections were incubated with the monoclonal antibody against CDV NP overnight at 4°C. The sections were washed and incubated with antibodies to the cell markers for 60 min at 37°C. The sections were washed and incubated with goat anti-rabbit IgG-Alexa Fluor 568 (Invitrogen) and goat anti-mouse IgG-Alexa Fluor 488 (Invitrogen) antibodies or donkey anti-goat IgG-Alexa Fluor 568 (Invitrogen) and donkey anti-mouse IgG-Alexa Fluor 488 (Invitrogen) antibodies for 60 min at 37°C. After being washed, the sections were mounted with SlowFade Gold antifade reagent with 4′,6-diamidino-2-phenylindole (DAPI) (Invitrogen). The images were captured by a fluorescence microscopy (IX71; Olympus) equipped with a Hamamatsu high-resolution digital black and white charge-coupled-device (CCD) camera (ORCA2; Hamamatsu Photonics).

Experimental infection of cynomolgus monkeys. Five cynomolgus monkeys of 5 to 11 years of age were obtained from the Tsukuba Primate Research Center (National Institute of Biomedical Innovation, Ibaraki, Japan). They were free from simian retrovirus type 4 (SRV) and were confirmed to be free from MV and CDV antibodies. Four of them (no. 4450, 4571, 4965, 4969) were male, while one (no. 4970) was female. Their cages were placed in negatively pressurized glove boxes. They were anesthetized with ketamine (0.1 ml/kg) and inoculated intranasally with 5×10^5 PFU of CDV in 0.5 ml of DMEM using a spray (0.25 ml in each nostril; Keytron). On the day of inoculation, and at 3, 7, 10, and 15 days after inoculation, body weight and body temperature were measured, and throat and rectal swabs and peripheral blood were obtained. PBMCs were isolated using Percoll gradients (GE Healthcare), adjusted to a concentration of 10^5/ml, and divided into 2-fold serial dilutions. Then, a 500-μl aliquot of each diluted PBMC sample was inoculated into Vero.DogSLAMtag cells. On the assumption that one CDV-infected PBMC was contained in the maximum diluted PBMC sample that induced syncytium, the number of CDV-infected PBMC/10^5 PBMCs was calculated. All monkeys were euthanized 15 days after inoculation by exsanguination under excess ketamine anesthesia, and tissue samples were collected for histopathological examination and virus isolation. For virus isolation, tissue homogenates were prepared in PBS containing antibiotics and clarified by centrifugation. These samples were inoculated to Vero.DogSLAMtag cells. When no cytopathic effect (CPE) was observed, RT-PCR was performed for the detection of CDV-specific RNAs. When no CDV-specific cDNA was amplified, samples were determined as being negative for CDV. Total numbers of blood cells were measured using an autoanalyzer (Cell Tuck; Nihon Koden). Numbers of neutrophils, lymphocytes, monocytes, eosinophils, and basophils were determined by microscopic analysis. A virus-neutralization test for CDV was performed using a plaque reduction method with a constant amount of virus and various serum dilution. Sample sera were serially diluted 4-fold and mixed with equal volumes of 100 PFU of CDV units. The neutralizing antibody titer was calculated at the 50% plaque reduction point by the Behrens-Kaerber method.

Multiplex analysis of cytokines and chemokines in monkey sera. Monkey sera were subjected to multiplex cytokine analysis using the human cytokine 25-plex antibody bead kit (Invitrogen) with Luminex 100 (Luminex Co.) according to the manufacturer's instructions. Enzyme-linked immunosorbent assays (ELISAs) were performed in duplicate, and the averages of each assay are shown.

Replication kinetics of the CDV isolate in Vero cells expressing SLAM and nectin4 of various animal species. Vero, Vero.DogSLAMtag, Vero/macSLAM, Vero/hSLAM, Vero/dNectin4, and Vero/macNectin4 cells (2×10^5 cells/well) were cultured in 24-well plates and infected with the CDV isolate at a multiplicity of infection (MOI) of 0.01. The cells were adsorbed with the virus for 1 h at 37°C, and then the virus inoculum was removed and the cells were rinsed twice with DMEM. The cells were cultured in DMEM supplemented with 1% fetal calf serum (FCS) at 37°C. The cells and culture supernatants were harvested every 12 h until 3 days postinfection (p.i.). The harvested samples were stored at −80°C until use. The samples were centrifuged at 1,000 × *g* and titrated with plaque assay.

Cell-to-cell fusion assay. DNA fragments encoding H and F protein of the CDV isolate were amplified by RT-PCR and cloned into the pCAGGS vector (18). Vero, Vero.DogSLAMtag, Vero/macSLAM, Vero/hSLAM, Vero/dNectin4, Vero/macNectin4, and Vero cells in 24-well plates were transfected with the F protein-expressing plasmid together with or without the H protein-expressing plasmid. To detect syncytia clearly, a fluorescent protein-expressing plasmid, pEGFP-C1 (Clontech Laboratories),

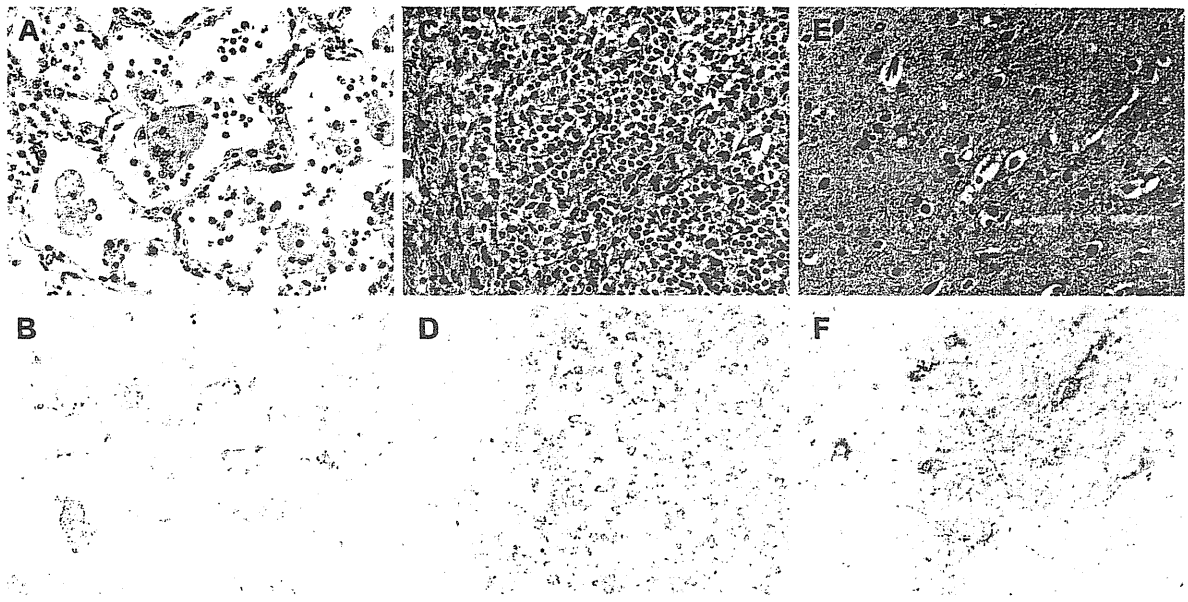

FIG 1 Histopathological analyses of cynomolgus monkeys naturally infected with CDV in the 2008 outbreak. Tissue sections obtained from cynomolgus monkey 11 were examined by hematoxylin and eosin staining (HE) and immunohistochemistry (IHC) using anti-CDV-NP monoclonal antibody. Giant cell pneumonia (A) and CDV antigen in the syncytial pneumocytes (B) were seen in the lung. Lymphocyte depletion (C) and CDV antigen in the mononuclear cells (D) were observed in the lymph node. Focal and slight microglia cell infiltration (E) and CDV antigen in neurons and glia cells (F) were observed in the cerebrum. HE, original magnification ×20; IHC, ×40.

was cotransfected. The cell monolayers were observed using an Axio Observer.D1 microscope at 16 and 24 h posttransfection.

Entry assay using pseudotyped viruses. To analyze the efficiency of virus entry using SLAM and nectin4 in more detail, a vesicular stomatitis virus (VSV) pseudotype system (17) was employed (VSVΔG* was kindly provided by M. A. Whitt, The University of Tennessee Health Science Center). A VSV pseudotype bearing the H protein and the F protein of the CDV strain on the surface of the virion (referred to as VSVΔG*-F-dVH) was constructed. VSV pseudotype bearing only the F protein (referred to as VSVΔG*-F) was also constructed. Vero, Vero.DogSLAMtag, Vero/macSLAM, Vero/dNectin4, and Vero/macNectin4 cells were infected with the VSV pseudotypes. Infectivity titers of the VSVΔG*-F-dVH and VSVΔG*-F were determined at 24 h p.i.

Ethics statement. The experiments with animals were performed at animal biological safety level 2 in strict accordance with the Animal Experimentation Guidelines of the National Institute of Infectious Diseases. The protocol was approved by the Institutional Animal Care and Use Committee of the institute (permit number 611001). Collection of the specimens from the monkeys was performed under ketamine hydrochloride anesthesia, and all efforts were made to minimize suffering.

RESULTS

Clinical and pathological features of cynomolgus monkeys naturally infected with CDV in the outbreak in Japan. Forty-six monkeys out of 432 cynomolgus monkeys died or were euthanized during a quarantine period after import from China in Japan in 2008, resulting in a fatality rate of 10.6% (46/432) if euthanized animals were considered to be fatal. Clinical signs of sick monkeys were characterized by eye mucus, nasal mucus, rhinitis, coughing, anorexia, diarrhea, fever, and generalized rash, which are similar to those observed in acute measles in humans and in monkeys in recent CDV outbreaks in China. Swelling of the footpads was also observed in sick monkeys. Three moribund monkeys were autopsied for histopathological examination. Histopathologically, two monkeys (animals 11 and 12) were in the acute phase of systemic CDV infection. One monkey (animal 13) was considered to be in a convalescent phase. Various stages of giant cell pneumonia were found in all three monkeys (Fig. 1A). CDV antigen-positive syncytial pneumocytes were seen in the lungs of two monkeys (animals 11 and 12) (Fig. 1B). In the thymus, spleen, tonsils, and lymph nodes of all monkeys, almost all lymphocytes were depleted, suggesting severe immune suppression. The remaining mononuclear cells were positive for CDV antigen in the lymph tissues of two monkeys (animals 11 and 12) (Fig. 1C and D). Focal gliosis and demyelination were found in the cerebrum and/or cerebellum of all monkeys. In these lesions, some neurons and glia cells were positive for CDV antigen in all monkeys (Fig. 1E and F). In other organs, including the skin, small and large intestines, kidneys, salivary glands, and testes, giant cells and/or CDV antigen-positive cells were observed. Interestingly, CDV antigen-positive cells were not observed in the tissues except for the brain and testis of monkey 13. The types of cells with CDV antigens in the tissues were identified by dual staining with antibodies to CDV NP and various cell markers (Fig. 2). CDV antigens were detected in some of the cytokeratin-positive giant cells in the bronchi and bronchiole (Fig. 2). The bronchiolar epithelial cells with CDV antigens were also necitin4 positive (Fig. 2). In addition, the virus antigens were also detected in the $CD3^+$ lymphocytes in the lymph node and the βIII tubulin-positive neurons in the brain (Fig. 2). Sera of the three monkeys (no. 11, 12, and 13) were subjected to multiplex cytokine analysis. Compared with eight normal monkeys from Tsukuba Primate Research Center, naturally CDV-infected monkeys in the outbreak showed upregulated levels of proinflammatory cytokines and chemokines, such as interleukin 1β (IL-1β), IL-6, macrophage inflammatory protein 1α (MIP-1α), MIP-1β, monocyte chemoattractant protein 1

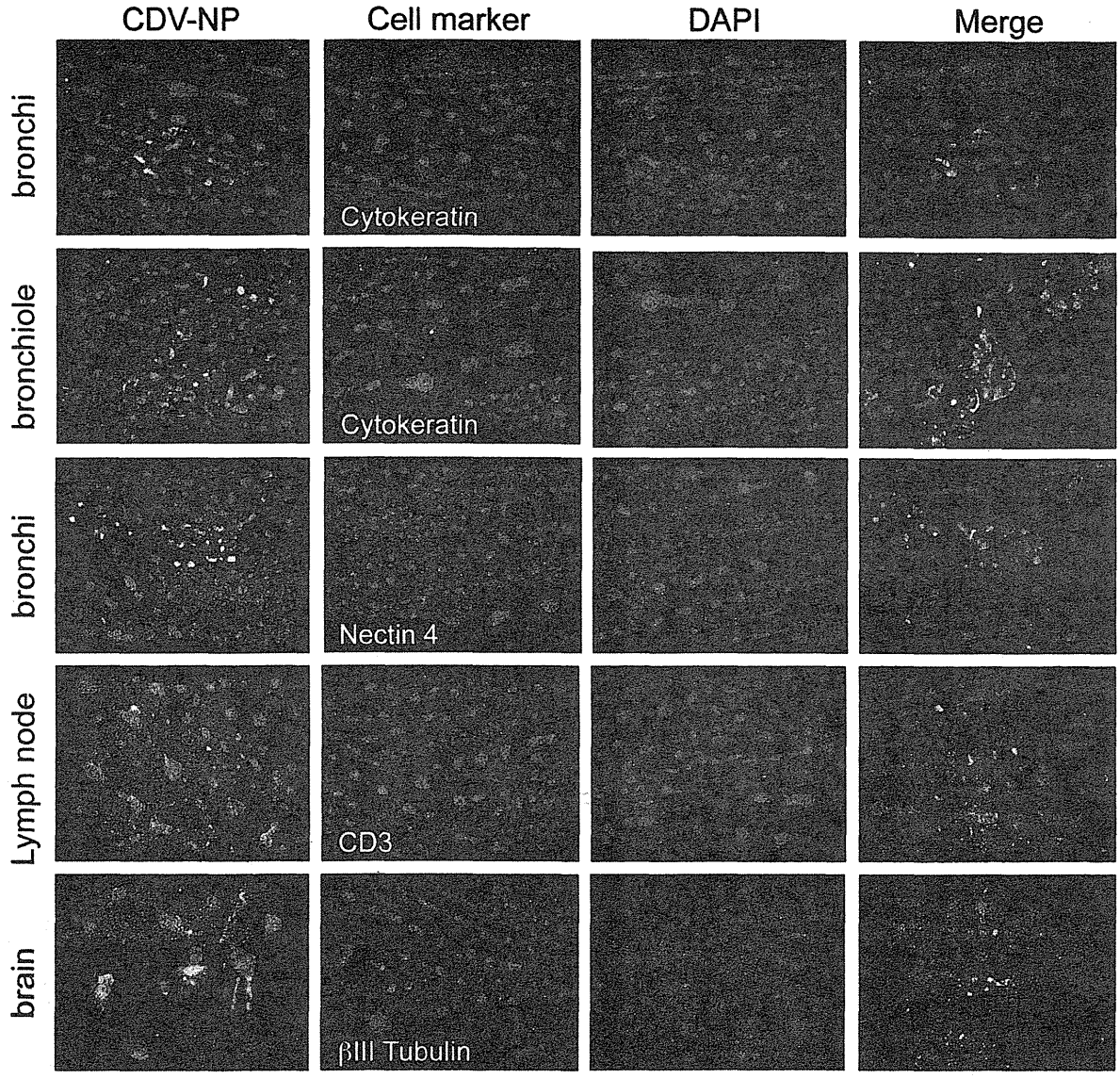

FIG 2 Double immunofluorescence staining of tissues of cynomolgus monkey 11 naturally infected with CDV in the 2008 outbreak. Tissue sections obtained from cynomolgus monkey 11 were examined by double immunofluorescence staining with anti-CDV-NP antibody and rabbit anti-cytokeratin, rabbit anti-neuron-specific β III tubulin, rabbit anti-CD3, or goat anti-nectin4 antibody. CDV-NP antigens were detected in the bronchi, bronchiole, lymph node, and brain. Some CDV-NP antigen-positive cells were positive for cytokeratin, nectin4, or CD3. A few CDV-NP antigen-positive neurons were positive for βIII tubulin.

(MCP-1), and eotaxin. Proinflammatory cytokines associated with T cell activation, gamma interferon (IFN-γ) and IL-15, were also found. Anti-inflammatory responses of IL-1 receptor antagonist (IL-1ra) were also upregulated in the monkeys (Table 1).

Isolation of CDV from monkeys using Vero.DogSLAMtag cells. Typical syncytia developed in monolayers of Vero.DogSLAMtag cells at as early as 2 days p.i. of spleen homogenates obtained from dead or moribund monkeys. However, syncytia were not observed in Vero cells inoculated with the spleen homogenates (data not shown). One of the CDV isolates was named CYN07-dV.

Relationship between CYN07-dV and Chinese CDV strains associated with monkey outbreaks. The entire genome nucleo-

TABLE 1 Blood chemokine/cytokine levels

Cytokine	Monkeys naturally infected with CDV			Normal monkeys			*P* value[a]
	Median (pg/ml)	*SD*	No. positive/ no. tested	Median (pg/ml)	*SD*	No. positive/ no. tested	
IL-1β	120	66	2/3	<17		0/8	0.023*
IL-6	94	72	3/3	<9		0/8	0.011*
MIP-1α	228	78	3/3	84	48	8/8	0.000**
MIP-1β	157	61	3/3	40	36	7/8	0.001**
MCP-1	3,917	2,286	3/3	461	245	8/8	0.043*
Eotaxin	2,121	1,096	3/3	413	203	8/8	0.023*
IFN-γ	509	150	3/3	261	183	3/8	0.002*
IL-15	89	65	2/3	64	23	1/8	0.115

[a] Asterisks indicate statistically significant differences between monkeys naturally infected with CDV and normal monkeys (*, $P < 0.05$; **, $P < 0.001$).

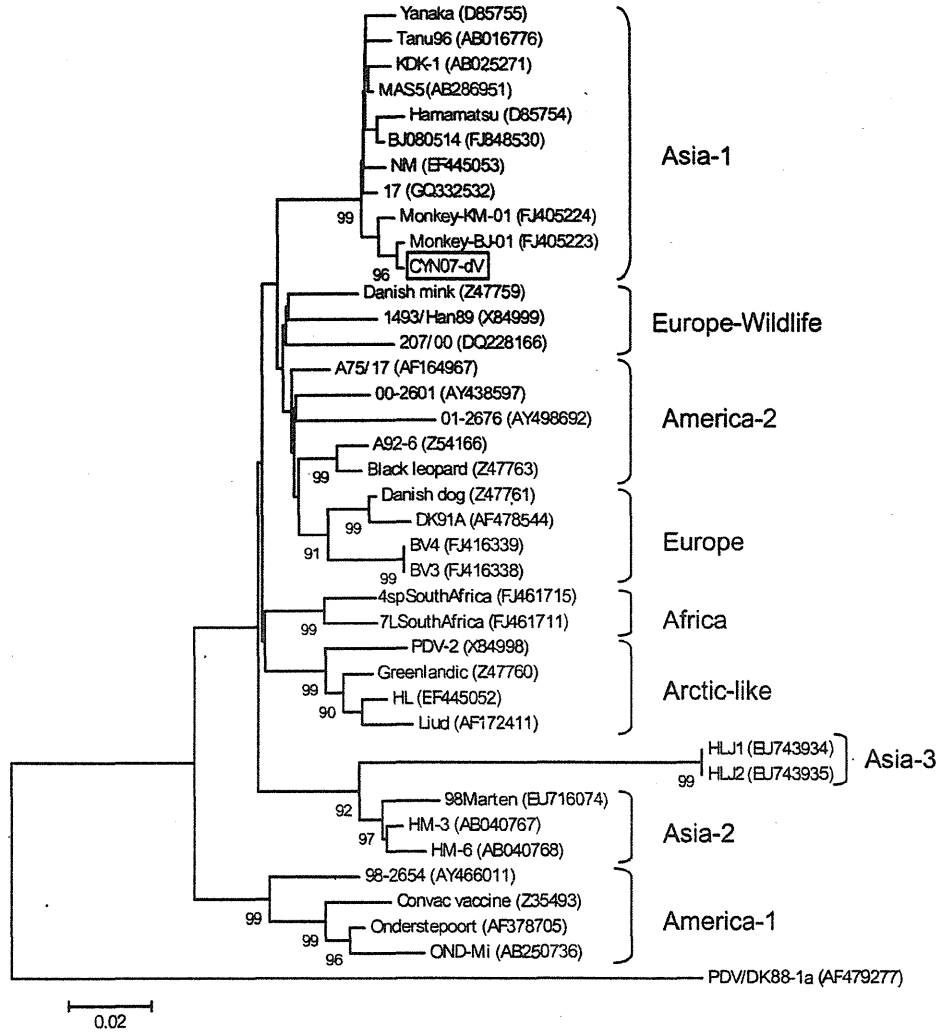

FIG 3 Phylogenetic tree of CDV based on the CYN07-dV sequence. Phylogenetic analysis of the H protein of the CDV showed that the CYN07-dV was closely related to the CDV strains isolated from rhesus monkeys in China. Scale bars indicate phylogenetic distance between CDV isolates.

tide sequence of the CDV strain CYN07-dV was determined (DDBJ/GenBank accession number AB687720). A phylogenic analysis of H protein indicated that CYN07-dV belongs to the Asia-1 clade and is closely related to monkey-BJ-01 and monkey-KM-01 strains (GenBank accession numbers FJ405223 and FJ405224, respectively) isolated from rhesus monkeys in China in 2008 (15) (Fig. 3). Comparative analyses throughout the genomes of CDV strains revealed that CYN07-dV showed the highest homology to the monkey-KM08 strain isolated from a rhesus monkey in China in 2008 (GenBank accession number HM852904) (15) (99.6%; 15,632/15,690 nucleotides). A phylogenic analysis indicated that CYN07-dV showed high homology with CDV isolates from different animal species in China (NM strain isolated from foxes in China and 17 strains isolated from dogs in China), suggesting a Chinese source of the CYN07-dV strain.

Experimental infection of cynomolgus monkeys with CYN07-dV. Five cynomolgus monkeys were infected intranasally with CYN07-dV. In these animals, no lethal infection was observed during an experimental period of 15 days, and clinical symptoms were less severe than those observed in the moribund and dead monkeys during the outbreak. However, all five monkeys had appetite loss at 7 to 12 days p.i. Body weight was decreased in three of the five monkeys (Fig. 4A). The rectal temperature was transiently increased at 3 to 7 days p.i. in some monkeys (Fig. 4B). In all five monkeys, the numbers of white blood cells and lymphocytes were decreased (Fig. 4C and D), as the numbers of CDV-infected PBMCs were increased (Fig. 4E). Neutralizing antibodies against CDV were detected in the monkey sera at 7 days p.i., and then the titers of antibodies were raised at 10 days p.i. (Fig. 4F). Infectious CDV was isolated from various tissues of autopsied specimens at 15 days p.i., including local lymph nodes, lungs, liver, kidneys, intestinal tracts, and central nervous tissues of monkeys (Table 2, 3). In monkey 4965, giant cells were observed in the alveolar area of the lungs where the syncytial pneumocytes were positive for CDV antigen (Fig. 5A and B), and lymphocytes were depleted in the lymph nodes where the follicular cells and mononuclear cells were positive for CDV antigen (Fig. 5C and D). These histopathological findings were also observed in

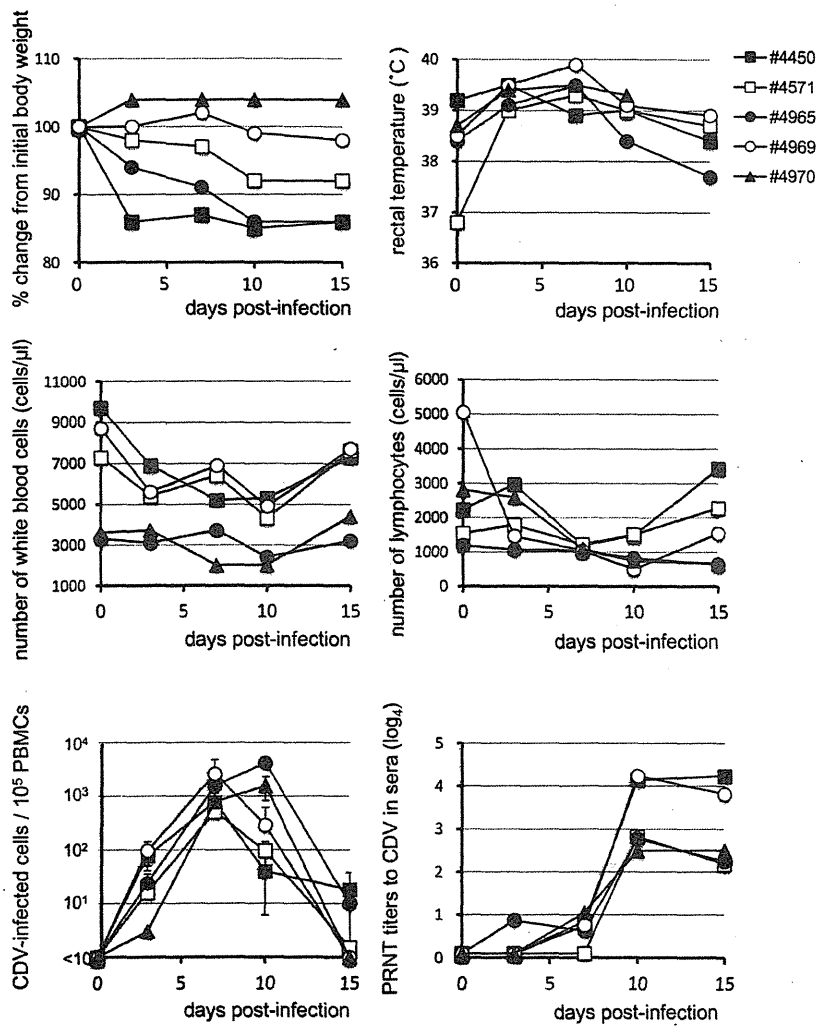

FIG 4 Changes in body weight, rectal temperature, and the numbers of white blood cells, lymphocytes, and CDV-infected PBMCs and neutralization antibody level in the experimentally CDV-infected monkeys. (A) Body weight; (B) rectal temperature; (C) white blood cell count; (D) lymphocytes count; (E) CDV-infected PBMC count; (F) neutralizing antibodies against CDV.

other monkeys but were less severe than those in monkey 4965 (data not shown). The experimentally CDV-infected monkeys showed upregulated levels of IFN-α and IL-1ra at 7 to 10 days p.i. Some monkeys showed upregulated levels of MIP-1β, MCP-1, eotaxin, IFN-γ, and IL-15 (data not shown).

The nucleotide and amino acid sequences of SLAM and nectin4 of cynomolgus monkeys. The nucleotide and deduced amino acid sequences of SLAM and nectin4 of cynomolgus monkeys were determined (DDBJ/GenBank accession numbers AB742520 and AB742522, respectively). Cynomolgus monkey

TABLE 2 CDV isolation from various organs in the experimentally infected cynomolgus monkeys at 15 days p.i.

	Result[a]									
Animal no.	Skin	Respiratory	Liver	Kidney	Intestine	Spleen	Lymph node[b]	Thymus	Tonsil	Central nervous system
4450	−	+	−	−	+	−	−	−	−	−
4571	−	+	−	−	+	+	+	+	+	−
4965	−	+	+	+	+	+	+	+	+	+
4969	−	−	−	−	−	−	−	−	−	−
4970	−	+	−	−	−	−	−	+	+	−

[a] −, CDV negative; +, CDV positive.
[b] Cervical and intestinal lymph node.

TABLE 3 CDV isolation from throat swabs, rectal swabs, and feces in the experimentally infected cynomolgus monkeys

	Result by day p.i.[a]																
	Throat swabs					Rectal swabs					Feces						
Animal no.	0	3	7	10	15	0	3	7	10	15	1–9	10	11	12	13	14	15
4450	−	−	−	−	−	−	−	+	+	−	−	−	+	+	−	−	−
4571	−	−	−	+	−	−	−	−	+	−	−	+	+	+	+	+	+
4965	−	−	−	+	+	−	−	−	+	−	−	+	+	−	+	+	+
4969	−	−	−	−	−	−	−	−	+	−	−	−	+	+	−	−	−
4970	−	−	−	−	−	−	−	−	−	−	−	−	−	−	−	−	−

[a] −, CDV negative; +, CDV positive.

SLAM showed high levels of identity to rhesus monkey SLAM (DDBJ/EMBL/GenBank accession no. XM_001117605) and human SLAM (DDBJ/EMBL/GenBank accession no. U33017), with 99.9% (100%) and 97.6% (96.7%) nucleotide (amino acid) identity, respectively. Amino acid sequences of the SLAM were completely conserved among three macaques: cynomolgus monkey, rhesus monkey, and pig-tailed monkey (AB742521) (data not shown). On the other hand, cynomolgus monkey SLAM showed a lower level of identity to dog SLAM (DDBJ/EMBL/GenBank accession no. AF390108), with 76.5% (65.0%) nucleotide (amino acid) identity.

Cynomolgus monkey nectin4 showed identity to dog nectin4 (DDBJ/EMBL/GenBank accession no. AB755429), rhesus monkey nectin4 (DDBJ/EMBL/GenBank accession no. XM_001117709), and human nectin4 (DDBJ/EMBL/GenBank accession no. NM_030916), with 89.0% (94.1%), 100% (100%), and 98.3% (99.4%) nucleotide (amino acid) identity, respectively.

CDV strain CYN07-dV utilizes macaca SLAM and macaca nectin4 as receptors. The replication kinetics of CYN07-dV was analyzed in Vero, Vero.DogSLAMtag, Vero/macSLAM, Vero/hSLAM, Vero/dNectin4, and Vero/macNectin4 cells. In Vero and Vero/hSLAM cells, CYN07-dV replicated inefficiently (Fig. 6A). On the other hand, it replicated efficiently in Vero.DogSLAMtag, Vero/macSLAM, Vero/dNectin4, and Vero/macNectin4 cells. The peak titer and replication kinetics of the virus in Vero/macSLAM cells were comparable to those in Vero.DogSLAMtag cells (Fig. 6A). The peak titer of the virus in Vero/macNectin4 cells was also comparable to that in Vero/dNectin4, although virus production was slightly delayed in Vero/macNectin4 cells (Fig. 6A). The wild-type CDV strain Ac96I (13), isolated from

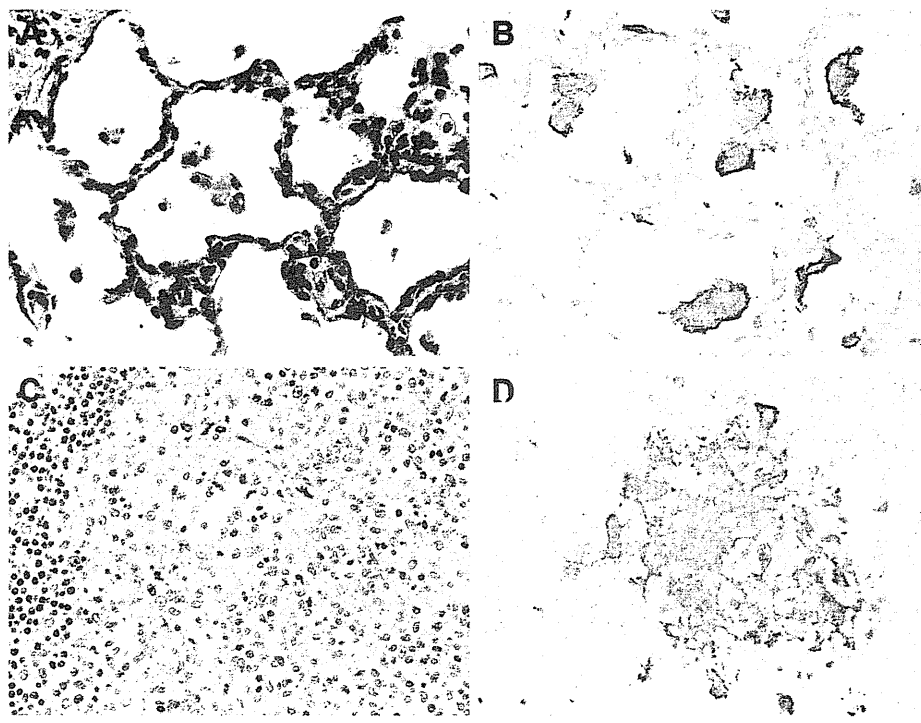

FIG 5 Histopathological analyses of cynomolgus monkeys experimentally infected with CDV. Tissue sections obtained from cynomolgus monkey 4965 were examined by hematoxylin and eosin staining and immunohistochemistry using anti-CDV-NP monoclonal antibody. Giant cells (A) with CDV antigen (B) were observed in the alveolar area in the lung. Lymphocyte depletion (C) and CDV antigen-positive cells were observed in the follicular area (D) in the lymph node of CYN07-dV-infected monkey 4965. HE, ×20; IHC, ×40.